Acta Mech (2007)
DOI 10.1007/s00707-007-0504-2
Printed in The Netherlands

Acta Mechanica

The composite Eshelby Tensors and their applications to homogenization

R. A. Sauer, G. Wang, S. Li

Department of Civil and Environmental Engineering, University of California, Berkeley, USA

Received 25 January 2007; Accepted 14 August 2007; Published online 14 November 2007

Summary. In recent studies, the exact solutions of the Eshelby tensors for a spherical inclusion in a finite, spherical domain have been obtained for both the Dirichlet- and Neumann boundary value problems, and they have been further applied to the homogenization of composite materials [15], [16]. The present work is an extension to a more general boundary condition, which allows for the continuity of both the displacement and traction field across the interface between RVE (representative volume element) and surrounding composite. A new class of Eshelby tensors is obtained, which depend explicitly on the material properties of the composite, and are therefore termed 'the Composite Eshelby Tensors'. These include the Dirichlet- and the Neumann-Eshelby tensors as special cases. We apply the new Eshelby tensors to the homogenization of composite materials, and it is shown that several classical homogenization methods can be unified under a novel method termed the 'Dual Eigenstrain Method'. We further propose a modified Hashin-Shtrikman variational principle, and show that the corresponding modified Hashin-Shtrikman bounds, like the Composite Eshelby Tensors, depend explicitly on the composite properties.

1 Introduction

Eshelby's solution for embedded inclusion problem [3]–[5] is fundamental in the development of contemporary micromechanics. In the past, numerous efforts have been made to extend Eshelby's solution to include the effects of material anisotropy [22], inclusion geometry [1], [25], imperfect interface conditions [8], non-uniform eigenstrains [21] and surface and interface energies [27].

Micromechanics is essentially a multiscale theory: Although a 'representative volume element' (RVE) can be viewed as a material point at the macro-scale, it is associated with specific microstructure at the micro-scale. It is well known that the classical Eshelby solution was obtained for an elastic isotropic inclusion embedded in an infinite elastic matrix. With uniform eigenstrain prescribed, the Eshelby tensor inside an elliptical or ellipsoidal inclusion is found as constant and size independent. The treatment of the RVE as an infinite space implies that the inclusion concentration is dilute, and therefore, a direct application of these results to the case of finite inclusion concentration is only approximate. To date, only limited work exists to study the inclusion problem for a finite RVE. It is not until recently that Li et al. [14]; Wang et al. [29]; Li et al [15]

Correspondence: Shaofan Li, Department of Civil and Environmental Engineering, University of California, Berkeley, CA94720, USA
e-mail: li@ce.berkeley.edu

utilized the invariant group properties of circular and spherical inclusions to derive the exact closed-form solutions of the Eshelby tensors for such inclusions within a finite RVE under both Dirichlet- and Neumann boundary conditions. It has been found that the so-called Dirichlet- and Neumann-Eshelby tensors are not constant tensors in the interior of the inclusion even for uniformly prescribed eigenstrains. Instead, they are dependent on the position inside the RVE and the volume fraction of the participating phases. They further have some salient symmetry properties denoted as 'transverse radial isotropy'. Consequently, the modification of existing homogenization methods [22], [23] via these finite Eshelby tensors provides significant improvement in predicting the behavior of composites [16]. In particular, the Hashin-Shtrikman variational bounds [6], [7] are modified according to the prescribed boundary condition.

The multiscale interaction of the microstructured RVE and its macroscopic environment can be more realistically represented by a three-phase model, where the finite RVE (inclusion and matrix) is geometrically idealized into concentric spheres (or circles in 2D) and is embedded in an infinite homogeneous and isotropic composite material. The three-phase model was used successfully in deriving the generalized self-consistent scheme (GSCS) [2] and improved Mori-Tanaka theory [18], [19] and it has been widely applied, for example, to study grain boundaries of poly-crystals [13], fiber or particle-reinforced composites [24], coated fiber composites [9], syntactic foams [20], and granular rock [26]. The elastic solution for the three phase model under uniform external load and under uniform eigenstrain were reported in [2] and [18], [19], however, these solutions are not all in closed-form and lack an expression for the Eshelby tensor.

In this paper, we extend our previous work to solve the exact elastic field and associated Eshelby tensor of an idealized, spherical, finite RVE embedded in an infinite, homogeneous, isotropic medium. This surrounding infinite medium can be identified with the homogenized composite and we therefore denote the boundary value problem of the RVE as the finite Eshelby problem under 'composite boundary conditions'. A solution is found which satisfies the continuity of the displacement and traction fields across the RVE/composite interface, and it is thus termed the 'Composite Eshelby Tensor'. It is shown that this result is a linear combination of the Dirichlet- and Neumann-Eshelby solutions reported in [15]. The fact that the 'Composite Eshelby Tensor' is a composition of these special results gives the terminology a twofold meaning. Second, we use the Composite Eshelby Tensor to explore its ramifications to existing homogenization techniques. A new scheme, termed the 'Dual Eigenstrain Method' is devised, which unifies previous homogenization methods. Third, we propose a new variational principle for the generalized boundary problem, such that the Hashin-Shtrikman bounds can be substantially modified. We note that the results presented here are all analytical and can be applied straightforwardly. In particular, we show that our model contains a closed-form result of the Modified Mori-Tanaka Method developed by Luo and Weng [18], [19].

The following Section serves as a brief review of our finite Eshelby tensor formalism, in particular the Dirichlet- and Neumann-Eshelby problems. They are needed for the development of the underlying concept, the 'Composite Eshelby problem', treated in Sect. 3. The important results of Sects. 2 and 3 are summarized in boxes 1, 2 and 3, so that one may skip the detailed derivation in preference for the following applications. These are the Dual Eigenstrain Method, discussed in Sect. 4, and the Modified Hashin-Shtrikman Bounds, derived in Sect. 5. We conclude this work in Sect. 6.

2 Dirichlet- and Neumann-Eshelby Tensors

In this section, a brief summary of the Dirichlet- and the Neumann-Eshelby tensors is outlined. For a detailed derivation, we refer to our original work [15]. The familiar reader may skip this section.

2.1 Considered problem

The problem under investigation is shown in Fig. 1. We consider a spherical inclusion Ω_I with radius a embedded at the center of a spherical RVE Ω with radius H_0. Consider two arbitrary points $\boldsymbol{x} \in \Omega$ and $\boldsymbol{y} \in \Omega$ and let $\boldsymbol{R} = \boldsymbol{y} - \boldsymbol{x}$. Each vector $\boldsymbol{x}, \boldsymbol{y}, \boldsymbol{R}$ can be expressed as its length multiplied by a unit direction vector. We shall denote these unit vectors as $\boldsymbol{r} = \boldsymbol{x}/|\boldsymbol{x}|$, $\boldsymbol{n} = \boldsymbol{y}/|\boldsymbol{y}|$ and $\ell = \boldsymbol{R}/R$, where $R = |\boldsymbol{R}|$. If $\boldsymbol{y}$ lies on the boundary, as shown in Fig. 1, we have $|\boldsymbol{y}| = H_0$ and $\boldsymbol{n}$ will be the outward normal of the boundary surface $\partial\Omega$. Furthermore we define the ratios $\rho = a/|\boldsymbol{x}|$, $\rho_0 = a/H_0$ and $t = |\boldsymbol{x}|/H_0 = \rho_0/\rho$ to allow for a non-dimensional description of the problem. An important quantity is the ratio between the volumes of the inclusion and the RVE, the so called volume fraction $f = \rho_0^3$. The material property of the inclusion Ω_I and the surrounding matrix $\Omega_E = \Omega/\Omega_I$ are given by the elastic tangents $\mathbb{C}^I$ and $\mathbb{C}^E$, which are considered as isotropic in the following derivation. It is noted that the concentric arrangement of the two phases, as shown in Fig. 1, is a chosen idealized representation of the true microstructure, which captures the volume fraction of the two phases within the RVE. The RVE is homogenized by considering the prescribed, piecewise constant eigenstrain distribution

$$\varepsilon^*(\boldsymbol{x}) = \begin{cases} \varepsilon^*, & \boldsymbol{x} \in \Omega_I, \\ 0, & \boldsymbol{x} \in \Omega_E, \end{cases} \tag{2.1}$$

such that the entire domain $\Omega = \Omega_I \cup \Omega_E$ has the constant modulus $\mathbb{C} = \mathbb{C}^E$. In passing, we note that this homogenization procedure may not be exactly the same as the classical "equivalent eigenstrain method" [22] since for a finite sphere the disturbance strain field due to a piecewise constant eigenstrain distribution is not uniform in general.

The displacement field $\boldsymbol{u}$ (and corresponding stress and strain fields $\boldsymbol{\sigma}, \boldsymbol{\varepsilon}$) within the RVE are decomposed into a background field $\boldsymbol{u}^0$ (and $\boldsymbol{\sigma}^0, \boldsymbol{\varepsilon}^0$), due to the far field boundary condition, and a disturbance field $\boldsymbol{u}^d$ (and $\boldsymbol{\sigma}^d, \boldsymbol{\varepsilon}^d$), due to the presence of the inclusion. Given the Green's Function for an infinite elastic domain

$$G_{ij}^{\infty}(\boldsymbol{x} - \boldsymbol{y}) = \frac{1}{16\pi\mu(1-\nu)}\left[\frac{(x_i - y_i)(x_j - y_j)}{R^3} + (3 - 4\nu)\frac{\delta_{ij}}{R}\right], \tag{2.2}$$

the solution of the disturbance displacement field can be expressed by the following integral equation:

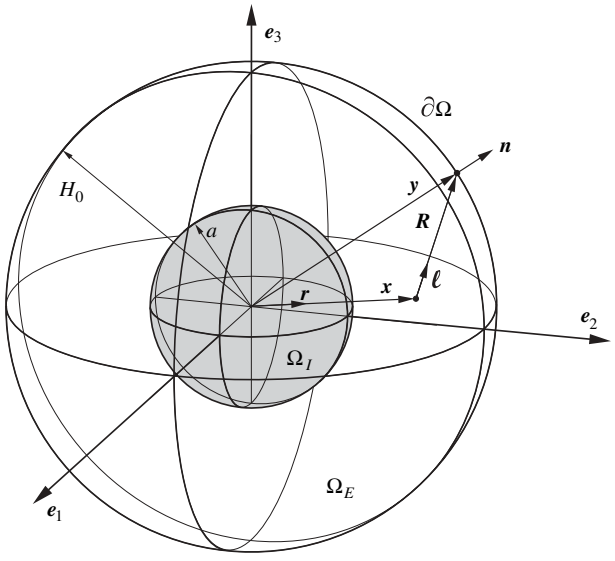

Fig. 1. Illustration of the single inclusion problem

$$u_m^d(\boldsymbol{x}) = -\int_{\Omega_I} \mathbb{C}^E_{ijk\ell} G^\infty_{im,j}(\boldsymbol{x}-\boldsymbol{y})\varepsilon^*_{k\ell}(\boldsymbol{y})d\Omega_y + \int_{\partial\Omega} t_i^d(\boldsymbol{y}) G^\infty_{im}(\boldsymbol{x}-\boldsymbol{y})dS_y + \int_{\partial\Omega} \mathbb{C}^E_{ijk\ell} u_k^d(\boldsymbol{y}) G^\infty_{im,j}(\boldsymbol{x}-\boldsymbol{y})\ n_\ell(\boldsymbol{y})dS_y, \quad \forall \boldsymbol{x},\boldsymbol{y} \in \Omega, \tag{2.3}$$

known as Somigliana's identity [28]. Here $t_i^d = \mathbb{C}^E_{ijk\ell}\varepsilon^d_{k\ell}n_j$ is the traction acting on the RVE surface. We emphasize that here and from now on μ and ν denote the shear modulus and Poisson's ratio of the *exterior* phase.

In the following we are interested in three special cases. The first arises when considering an infinite RVE. Dropping the boundary terms we arrive at the expression

$$u_i^d(\boldsymbol{x}) = -\int_{\Omega_I} \mathbb{C}^E_{k\ell mn} G^\infty_{ik,\ell}(\boldsymbol{x}-\boldsymbol{y})\varepsilon^*_{mn}(\boldsymbol{y})d\Omega_y, \tag{2.4}$$

which gives rise to the infinite Eshelby tensors denoted as $\mathbb{S}^{I,\infty}$ for $\boldsymbol{x} \in \Omega_I$ and $\mathbb{S}^{E,\infty}$ for $\boldsymbol{x} \in \Omega_E$.

Second, we consider the prescribed macrostrain boundary condition $\boldsymbol{u} = \boldsymbol{\varepsilon}^0\boldsymbol{x}, \forall \boldsymbol{x} \in \partial\Omega$ which implies the Dirichlet problem $\boldsymbol{u}^d = 0$ on $\partial\Omega$, so that expression (2.3) becomes

$$u_m^d(\boldsymbol{x}) = -\int_{\Omega_I} \mathbb{C}^E_{ijk\ell} G^\infty_{im,j}\varepsilon^*_{k\ell}d\Omega_y + \int_{\partial\Omega} \mathbb{C}^E_{ijk\ell} u^d_{k,\ell} G^\infty_{im} n_j dS_y. \tag{2.5}$$

We will see that this integral equation gives rise to the Dirichlet-Eshelby tensors $\mathbb{S}^{I,D}$ for $\boldsymbol{x} \in \Omega_I$ and $\mathbb{S}^{E,D}$ for $\boldsymbol{x} \in \Omega_E$.

Finally, by considering the prescribed macrostress boundary condition $\boldsymbol{t} = \boldsymbol{\sigma}^0\boldsymbol{n}, \forall \boldsymbol{x} \in \partial\Omega$, we obtain the Neumann problem $\boldsymbol{t}^d = 0$ on $\partial\Omega$. Then expression (2.3) becomes

$$u_m^d(\boldsymbol{x}) = -\int_{\Omega_I} \mathbb{C}^E_{ijk\ell} G^\infty_{im,j}\varepsilon^*_{k\ell}d\Omega_y + \int_{\partial\Omega} \mathbb{C}^E_{ijk\ell} u^d_k G^\infty_{im,j} n_\ell dS_y, \tag{2.6}$$

which leads to the Neumann-Eshelby tensors $\mathbb{S}^{I,N}$ for $\boldsymbol{x} \in \Omega_I$ and $\mathbb{S}^{E,N}$ for $\boldsymbol{x} \in \Omega_E$.

2.2 The Eshelby tensor decomposition

The infinite, Dirichlet- or Neumann-Eshelby tensor $\mathbb{S}^{\bullet,*}$ ($\bullet = I$ or E; $* = \infty$, D or N) relate the disturbance strain $\boldsymbol{\varepsilon}^d$ to the prescribed eigenstrain $\boldsymbol{\varepsilon}^*$ as

$$\varepsilon^d_{ij}(\boldsymbol{x}) = \mathbb{S}^{\bullet,*}_{ijmn}(\boldsymbol{x})\varepsilon^*_{mn}, \quad \forall \boldsymbol{x} \in \Omega. \tag{2.7}$$

It has been shown in [15] that the Eshelby tensor, which depends on $\boldsymbol{x} = tH_0\,\boldsymbol{r}$, can be decomposed into

$$\mathbb{S}_{ijmn}(\boldsymbol{x}) = \boldsymbol{S}(t) \cdot \boldsymbol{\Theta}_{ijmn}(\boldsymbol{r}), \tag{2.8}$$

a dot product between the two arrays

$$\mathbf{S}(t) := \begin{bmatrix} S_1(t) \\ S_2(t) \\ S_3(t) \\ S_4(t) \\ S_5(t) \\ S_6(t) \end{bmatrix}, \quad \boldsymbol{\Theta}_{ijmn}(\boldsymbol{r}) := \begin{bmatrix} \delta_{ij}\delta_{mn} \\ \delta_{im}\delta_{jn} + \delta_{in}\delta_{jm} \\ \delta_{ij}r_m r_n \\ \delta_{mn}r_i r_j \\ \delta_{im}r_j r_n + \delta_{in}r_j r_m + \delta_{jm}r_i r_n + \delta_{jn}r_i r_m \\ r_i r_j r_m r_n \end{bmatrix}. \tag{2.9}$$

Since $\mathbf{S}$ depends on the radial distance, t, of point $\boldsymbol{x}$, $\mathbf{S}$ is also denoted as the radial basis of $\mathbb{S}$, and since $\boldsymbol{\Theta}_{ijmn}$ depends on the radial direction, $\boldsymbol{r}$, of point $\boldsymbol{x}, \boldsymbol{\Theta}_{ijmn}$ is also referred to as the circumference basis of $\mathbb{S}$.

Similar to relation (2.7) we can identify a third order tensor $\mathbb{U}^{\bullet,*}$, which relates the disturbance displacement field $\boldsymbol{u}^d$ to the prescribed eigenstrain $\boldsymbol{\varepsilon}^*$ as

$$u_i^d(\boldsymbol{x}) = \mathbb{U}_{imn}^{\bullet,*}(\boldsymbol{x})\varepsilon_{mn}^*, \quad \forall \boldsymbol{x} \in \Omega. \tag{2.10}$$

The tensor $\mathbb{U}$ admits the decomposition

$$\mathbb{U}_{imn}(\boldsymbol{x}) = \mathbf{U}(t) \cdot \boldsymbol{\Xi}_{imn}(\boldsymbol{r}), \tag{2.11}$$

a dot product between the two arrays

$$\mathbf{U}(t) = \begin{bmatrix} U_1(t) \\ U_2(t) \\ U_3(t) \end{bmatrix}, \quad \boldsymbol{\Xi}_{imn}(\boldsymbol{r}) := \begin{bmatrix} r_i\delta_{mn} \\ r_m\delta_{in} + r_n\delta_{im} \\ r_i r_m r_n \end{bmatrix}. \tag{2.12}$$

Due to their arguments we call $\mathbf{U}$ the radial basis and Ξ_{imn} the circumference basis of $\mathbb{U}$. The strain-displacement relation

$$\varepsilon_{ij}^d = \frac{1}{2}(u_{i,j}^d + u_{j,i}^d) \tag{2.13}$$

establishes a direct link between the coefficients $\mathbf{U}$ and $\mathbf{S}$. Given $\mathbf{U}$ the strain coefficients $\mathbf{S}$ can be uniquely obtained from

$$\mathbf{S}(t) = \mathfrak{D}(t)\mathbf{U}(t), \tag{2.14}$$

where $\mathfrak{D}$ is the derivative operator

$$\mathfrak{D}(t) = \frac{1}{H_0}\begin{bmatrix} \frac{1}{t} & 0 & 0 \\ 0 & \frac{1}{t} & 0 \\ 0 & 0 & \frac{1}{t} \\ -\frac{1}{t} + \frac{d}{dt} & 0 & 0 \\ 0 & -\frac{1}{2t} + \frac{1}{2}\frac{d}{dt} & \frac{1}{2t} \\ 0 & 0 & -\frac{3}{t} + \frac{d}{dt} \end{bmatrix}. \tag{2.15}$$

Likewise given $\mathbf{S}$ the displacement coefficients $\mathbf{U}$ follow from

$$\mathbf{U}(t) = \mathfrak{I}(t)\mathbf{S}(t), \tag{2.16}$$

where $\mathfrak{I}$ is the integration operator

$$\mathfrak{I}(t) = H_0 t \begin{bmatrix} 1 & 0 & 0 & 0 & 0 & 0 \\ 0 & 1 & 0 & 0 & 0 & 0 \\ 0 & 0 & 1 & 0 & 0 & 0 \end{bmatrix}. \tag{2.17}$$

We remark that the displacements are only uniquely determinable from the strains up to a rigid body displacement, which is set to zero here.

2.3 The infinite problem

Let us now consider the solution of the infinite problem (2.4). Considering (2.13), (2.7) and (2.10) expression (2.4) can be written as

$$\begin{aligned} u_i^d(\boldsymbol{x}) &= \mathbb{U}_{imn}^{\bullet,\infty}\varepsilon_{mn}^*, \quad \mathbb{U}_{imn}^{\bullet,\infty} = -\int\limits_{\Omega_I} \mathbb{C}_{k\ell mn}^E G_{ik,\ell}^{\infty}(\boldsymbol{x}-\boldsymbol{y})d\Omega_y, \\ \varepsilon_{ij}^d(\boldsymbol{x}) &= \mathbb{S}_{ijmn}^{\bullet,\infty}\varepsilon_{mn}^*, \quad \mathbb{S}_{ijmn}^{\bullet,\infty} = -\frac{1}{2}\int\limits_{\Omega_I} \Big(\mathbb{C}_{k\ell mn}^E G_{ik,\ell j}^{\infty}(\boldsymbol{x}-\boldsymbol{y}) + \mathbb{C}_{k\ell mn}^E G_{jk,\ell i}^{\infty}(\boldsymbol{x}-\boldsymbol{y})\Big)d\Omega_y. \end{aligned} \tag{2.18}$$

The evaluation of $\mathbb{U}$ and $\mathbb{S}$ takes two forms ($\bullet = I$ or $\bullet = E$) depending on the location of $\boldsymbol{x}$. For the spherical inclusion Ω_I, the tensors $\mathbb{U}^{I,\infty}, \mathbb{U}^{E,\infty}$ and $\mathbb{S}^{I,\infty}, \mathbb{S}^{E,\infty}$ can be written as

$$\mathbb{U}_{imn}^{\bullet,\infty}(\boldsymbol{x}) = \mathbf{U}^{\bullet,\infty}(t)\cdot\boldsymbol{\Xi}_{imn}(\mathbf{r}), \quad \mathbb{S}_{ijmn}^{\bullet,\infty}(\boldsymbol{x}) = \mathbf{S}^{\bullet,\infty}(t)\cdot\boldsymbol{\Theta}_{ijmn}(\mathbf{r}), \tag{2.19}$$

where the radial arrays $\mathbf{U}^{I,\infty}$, $\mathbf{U}^{E,\infty}$ and $\mathbf{S}^{I,\infty}$, $\mathbf{S}^{E,\infty}$ are given explicitly in Appendix A.

2.4 The Dirichlet problem

To solve the Dirichlet problem we write Somigliana's identity (2.5) as

$$\begin{aligned} \varepsilon_{ij}^d(\boldsymbol{x}) = &-\frac{1}{2}\int\limits_{\Omega_I} \mathbb{C}_{k\ell mn}^E\Big(G_{ki,\ell j}^{\infty}(\boldsymbol{x}-\boldsymbol{y}) + G_{kj,\ell i}^{\infty}(\boldsymbol{x}-\boldsymbol{y})\Big)d\Omega_y\ \varepsilon_{mn}^* \\ &+\frac{1}{2}\int\limits_{\partial\Omega} \mathbb{C}_{k\ell mn}^E\varepsilon_{mn}^d(\boldsymbol{y})\Big(G_{ki,j}^{\infty}(\boldsymbol{x}-\boldsymbol{y}) + G_{kj,i}^{\infty}(\boldsymbol{x}-\boldsymbol{y})\Big)n_\ell(\boldsymbol{y})dS_y, \end{aligned} \tag{2.20}$$

an integral equation in terms of the unknown disturbance strain field $\boldsymbol{\varepsilon}^d$. It can be solved exactly by supposing the relation

$$\varepsilon_{ij}^d(\boldsymbol{x}) = \mathbb{S}_{ijk\ell}^{\bullet,D}(\boldsymbol{x})\varepsilon_{k\ell}^*, \quad \forall\boldsymbol{x}\in\Omega, \tag{2.21}$$

to hold for the Dirichlet-Eshelby tensor $\mathbb{S}^{\bullet,D}$. Substituting Eq. (2.21) into (2.20) and canceling $\boldsymbol{\varepsilon}^*$, we can write

$$\mathbb{S}_{ijmn}^{\bullet,D}(\boldsymbol{x}) = \mathbb{S}_{ijmn}^{\bullet,\infty}(\boldsymbol{x}) + \mathbb{S}_{ijmn}^{B,D}(\boldsymbol{x}), \tag{2.22}$$

where we have defined the Dirichlet boundary contribution

$$\mathbb{S}_{ijmn}^{B,D}(\boldsymbol{x}) := \frac{1}{2}\int\limits_{\partial\Omega} \mathbb{C}_{k\ell st}^E\mathbb{S}_{stmn}^{E,D}(\boldsymbol{y})\left(G_{ki,j}^{\infty}(\boldsymbol{x}-\boldsymbol{y}) + G_{kj,i}^{\infty}(\boldsymbol{x}-\boldsymbol{y})\right)n_\ell(\boldsymbol{y})dS_y. \tag{2.23}$$

Due to decomposition (2.8), Eq. (2.22) can be written as a relation for the radial basis arrays $\mathbf{S}$. Considering the two cases ($\bullet = I$ or E) we thus obtain

$$\mathbf{S}^{I,D}(t) = \mathbf{S}^{I,\infty}(t) + \mathbf{S}^{B,D}(t), \quad 0\le t<\rho_0, \tag{2.24.1}$$

$$\mathbf{S}^{E,D}(t) = \mathbf{S}^{E,\infty}(t) + \mathbf{S}^{B,D}(t), \quad \rho_0\le t\le 1. \tag{2.24.2}$$

We have shown in [15] that, by supplying $\mathbb{S}_{ijmn}^{B,D}(\boldsymbol{x}) = \mathbf{S}^{B,D}(t)\cdot\boldsymbol{\Theta}_{ijmn}(\boldsymbol{r})$ and $\mathbb{S}_{ijmn}^{E,D}(\boldsymbol{y}) = \mathbf{S}^{E,D}(1)\cdot\boldsymbol{\Theta}_{ijmn}(\boldsymbol{n})$, Eq. (2.23) can be integrated exactly to provide a relation between $\mathbf{S}^{B,D}$ and $\mathbf{S}^{E,D}$, namely

$$\mathbf{S}^{B,D}(t) = \mathbf{K}_D(t)\mathbf{S}^{E,D}(1). \tag{2.25}$$

Here $\mathbf{K}_D(t) = \mathbf{K}_2(t)\,\mathbf{K}_1$ is a (6 × 6) matrix factorized into the contributions

$$\mathbf{K}_1 = \mu \begin{bmatrix} \frac{2+2v}{1-2v} & \frac{4v}{1-2v} & 0 & \frac{2(1-v)}{1-2v} & 0 & 0 \\ 0 & 2 & 0 & 0 & 2 & 0 \\ 0 & 0 & \frac{2+2v}{1-2v} & 0 & \frac{4}{1-2v} & \frac{2(1-v)}{1-2v} \end{bmatrix} \tag{2.26}$$

and

$$\mathbf{K}_2(t) = \frac{-1}{420\mu(1-v)} \begin{bmatrix} 70(2v-1) & 28 & 4v(7-3t^2) \\ 0 & 28(5v-4) & 7(4v-5)+3t^2(7-4v) \\ 0 & 0 & 6t^2(10v-7) \\ 0 & 0 & -24vt^2 \\ 0 & 0 & 18vt^2 \\ 0 & 0 & 0 \end{bmatrix}. \tag{2.27}$$

Substituting Eq. (2.25) into (2.24.2) and evaluating it at $t = 1$ furnishes an equation for $\mathbf{S}^{E,D}(1)$,

$$\mathbf{S}^{E,D}(1) = [\mathbf{I}_6 - \mathbf{K}_D(1)]^{-1}\mathbf{S}^{E,\infty}(1), \tag{2.28}$$

where $\mathbf{I}_6$ is the (6 × 6) identity matrix. The solution of this equation together with Eqs. (2.25) and (2.24) solves the Dirichlet-Eshelby problem. The explicit expression of the Dirichlet boundary contribution $\mathbf{S}^{B,D}(t)$ is given in Appendix A. A summary of the Dirichlet-Eshelby tensor is given in Box 1.

The disturbance displacement field, as characterized by Eq. (2.10), now follows from the application of Eq. (2.16). We thus obtain the description of $\boldsymbol{u}^d$ as summarized in Box 2, which can be seen in analogy to Box 1.

2.5 The Neumann problem

The Neumann BVP Problem (2.6), an integral equation in u_i^d, can be solved directly on the displacement level. Considering the decomposition

$$u_i^d(\boldsymbol{x}) = \mathbb{U}_{imn}^{\bullet,N}(\boldsymbol{x})\,\varepsilon_{mn}^*, \tag{2.29}$$

Eq. (2.6) can be written as

$$\mathbb{U}_{imn}^{\bullet,N}(\boldsymbol{x}) = \mathbb{U}_{imn}^{\bullet,\infty}(\boldsymbol{x}) + \mathbb{U}_{imn}^{B,N}(\boldsymbol{x}), \tag{2.30}$$

where we have defined the Neumann boundary contribution

Box 1. Dirichlet- and Neumann-Eshelby tensors

Dirichlet- and Neumann-Eshelby relation
$\varepsilon_{ij}^d = \mathbb{S}_{ijmn}^{\bullet,*}\varepsilon_{mn}^*, \quad (\bullet = I,E;\ * = D,N)$

Radial and circumference basis decomposition
$\mathbb{S}_{ijmn}^{\bullet,*}(\boldsymbol{x}) = \mathbf{S}^{\bullet,*}(t) \cdot \boldsymbol{\Theta}_{ijmn}(\boldsymbol{r}), \quad \boldsymbol{\Theta}_{ijmn}(\boldsymbol{r})$ from (2.9)

Radial basis equations
$\mathbf{S}^{I,*}(t) = \mathbf{S}^{I,\infty}(t) + \mathbf{S}^{B,*}(t), \quad 0 \le \mathrm{t} < \rho_0,$
$\mathbf{S}^{E,*}(t) = \mathbf{S}^{E,\infty}(t) + \mathbf{S}^{B,*}(t), \quad \rho_0 \le t \le 1.$

Coefficients $\mathbf{S}^{I,\infty}$, $\mathbf{S}^{E,\infty}$, $\mathbf{S}^{B,D}$ and $\mathbf{S}^{B,N}$ are given in Appendix A for the 3D spherically symmetric case

Box 2. Dirichlet and Neumann disturbance displacement fields

Dirichlet and Neumann disturbance displacement field

$u_i^d = \mathbb{U}_{imn}^{\bullet,*}\varepsilon_{mn}^*, \quad (\bullet = I,E;\ * = D,N)$

Radial and circumference basis decomposition

$\mathbb{U}_{imn}^{\bullet,*}(\boldsymbol{x}) = \mathbf{U}^{\bullet,*}(t)\cdot\boldsymbol{\Xi}_{imn}(\boldsymbol{r}) \quad \boldsymbol{\Xi}_{imn}(\boldsymbol{r})$ from (2.12)

Radial basis equations

$\mathbf{U}^{I,*}(t) = \mathbf{U}^{I,\infty}(t) + \mathbf{U}^{B,*}(t), \quad 0 \le \mathrm{t} < \rho_0,$

$\mathbf{U}^{E,*}(t) = \mathbf{U}^{E,\infty}(t) + \mathbf{U}^{B,*}(t),$

Coefficients $\mathbf{U}^{I,\infty}$, $\mathbf{U}^{E,\infty}$, $\mathbf{U}^{B,D}$ and $\mathbf{U}^{B,N}$ are given in Appendix A for the 3D spherically symmetric case

$$\mathbb{U}_{imn}^{B,N}(\boldsymbol{x}) := \int_{\partial\Omega} \mathbb{C}_{k\ell st}\ \mathbb{U}_{smn}^{E,N}\, G_{ki,\ell}^{\infty}(\boldsymbol{x}-\boldsymbol{y})\ n_t(\boldsymbol{y})dS_y. \tag{2.31}$$

Due to decomposition (2.11), Eq. (2.30) can be written as a relation between the radial basis arrays $\boldsymbol{U}$, which is

$$\mathbf{U}^{I,N}(t) = \mathbf{U}^{I,\infty}(t) + \mathbf{U}^{B,N}(t), \quad 0 \le t < \rho_0, \tag{2.32.1}$$

$$\mathbf{U}^{E,N}(t) = \mathbf{U}^{E,\infty}(t) + \mathbf{U}^{B,N}(t), \quad \rho_0 \le t \le 1. \tag{2.32.2}$$

Substituting $\mathbb{U}_{imn}^{B,N}(\boldsymbol{x}) = \mathbf{U}^{B,N}(t)\cdot\boldsymbol{\Xi}_{imn}(\boldsymbol{r})$ and $\mathbb{U}_{imn}^{E,N}(\boldsymbol{y}) = \mathbb{U}^{E,N}(1)\cdot\boldsymbol{\Xi}_{imn}(\boldsymbol{n})$ into Eq. (2.31) and performing the integration, we can find the relation [15]

$$\mathbf{U}^{B,N}(t) = \mathbf{K}_N(t)\mathbf{U}^{E,N}(1), \tag{2.33}$$

with

$$\mathbf{K}_N(t) = \frac{t}{1-\nu}\begin{bmatrix} \dfrac{2(1-2\nu)}{3} & \dfrac{2(1-5\nu)}{15} & \dfrac{-2\nu(7-4t^2)}{35} \\ 0 & \dfrac{7-5\nu}{15} & \dfrac{7(5-\nu)+6t^2(4\nu-7)}{105} \\ 0 & 0 & \dfrac{4(7-10\nu)t^2}{35} \end{bmatrix}. \tag{2.34}$$

Substituting (2.33) into (2.32.2) at $t = 1$ gives an expression for $\mathbf{U}^{E,N}(1)$, namely

$$\mathbf{U}^{E,N}(1) = [\mathbf{I}_3 - \mathbf{K}_N(1)]^{-1}\mathbf{U}^{E,\infty}(1), \tag{2.35}$$

where $\mathbf{I}_3$ is the 3 $\times$ 3 identity matrix. The solution of this equation together with Eqs. (2.33) and (2.32) solves the Neumann-Eshelby Problem. The explicit expression of the Neumann boundary contribution $\mathbf{U}^{B,N}(t)$ is given in Appendix A. The disturbance strain field according to (2.7) now follows from differentiation of (2.14). A summary of the disturbance strain and displacement fields can be found in Boxes 1 and 2.

2.6 The traction field

Finally, for the derivation of the composite finite Eshelby Tensors in Sect. 3, we need to discuss the traction field. We introduce the disturbance traction field $\boldsymbol{t}^d$ acting on the surface defined by the outward unit normal $\boldsymbol{r}$, i.e., the surface of any sphere placed concentrically within the RVE. In terms of the prescribed eigenstrain $\boldsymbol{\varepsilon}^*$ this traction is given, for both the Dirichlet and the Neumann problem (* = D, N), as

$$t_i^d(\boldsymbol{x}) := \sigma_{ij}^d(\boldsymbol{x})\, r_j(\boldsymbol{x}) = \begin{cases} \mathbb{C}^E_{ijk\ell}\Big(\mathbb{S}^{I,*}_{k\ell mn}(\boldsymbol{x}) - \mathbb{I}^s_{k\ell mn}\Big) r_j(\boldsymbol{x})\, \varepsilon^*_{mn}, & \forall \boldsymbol{x} \in \Omega_I, \\ \mathbb{C}^E_{ijk\ell}\ \mathbb{S}^{E,*}_{k\ell mn}(\boldsymbol{x})\ r_j(\boldsymbol{x})\ \varepsilon^*_{mn}, & \forall \boldsymbol{x} \in \Omega_E, \end{cases} \tag{2.36}$$

where $\mathbb{I}^s$ is the fourth order identity tensor which can be written as $\mathbb{I}^s_{ijmn} = \mathbf{I}^s \cdot \boldsymbol{\Theta}_{ijmn}$, for $\mathbf{I}^s = [0,\ 1/2,\ 0,\ 0,\ 0,\ 0]^T$, and $\boldsymbol{\Theta}_{ijmn}$ is given by Eq. (2.9). In analogy to the preceding developments we can write the traction as

$$t_i^d(\boldsymbol{x}) = \mathbb{T}^{\bullet,*}_{imn}(\boldsymbol{x})\, \varepsilon^*_{mn}, \quad \begin{array}{l} \mathbb{T}^{I,*}_{imn}(\boldsymbol{x}) := \mathbb{C}_{ijkl}\Big(\mathbb{S}^{I,*}_{klmn}(\boldsymbol{x}) - \mathbb{I}^s_{k\ell mn}\Big) r_j(\boldsymbol{x}), \\ \mathbb{T}^{E,*}_{imn}(\boldsymbol{x}) := \mathbb{C}_{ijkl}\, \mathbb{S}^{E,*}_{klmn}(\boldsymbol{x})\ r_j(\boldsymbol{x}), \end{array} \tag{2.37}$$

where we have introduced the third order tensor $\mathbb{T}$ which can be decomposed as

$$\mathbb{T}_{imn}(\boldsymbol{x}) = \mathbf{T}(t) \cdot \boldsymbol{\Xi}_{imn}(\boldsymbol{r}), \tag{2.38}$$

with $\mathbf{T}(t) = [T_1(t),\ T_2(t),\ T_3(t)]$ and $\boldsymbol{\Xi}_{imn}$ given by Eq. (2.12).

Equations (2.38), (2.37) and (2.8) provide the relation between the arrays $\mathbf{T}^{\bullet,*}$ and $\mathbf{S}^{\bullet,*}$, namely the matrix equations

$$\mathbf{T}^{I,*}(t) = \mathbf{K}_1 \left[\mathbf{S}^{I,*}(t) - \mathbf{I}^s\right], \quad \mathbf{T}^{E,*}(t) = \mathbf{K}_1 \mathbf{S}^{E,*}(t), \tag{2.39}$$

where $\mathbf{K}_1$ is given by Eq. (2.26). In view of Box 1 we can thus write

$$\begin{aligned} &\mathbf{T}^{I,*}(t) = \mathbf{T}^{I,\infty}(t) + \mathbf{T}^{B,*}(t) - \mathbf{T}^*, \quad 0 \le t < \rho_0, \\ &\mathbf{T}^{E,*}(t) = \mathbf{T}^{E,\infty}(t) + \mathbf{T}^{B,*}(t), \quad \rho_0 \le t \le 1, \end{aligned} \tag{2.40}$$

where $\mathbf{T}^{I,\infty}$, $\mathbf{T}^{E,\infty}$, $\mathbf{T}^{B,D}$, $\mathbf{T}^{B,N}$ and $\mathbf{T}^* = \mathbf{K}_1\ \mathbf{I}^s$ are given in Appendix A.

3 Composite Eshelby tensors

In the preceding section we have solved Somigliana's identity considering either a pure Dirichlet problem, $\boldsymbol{u}^d = 0$ on $\partial\Omega$, or a pure Neumann problem, $\boldsymbol{t}^d = 0$ on $\partial\Omega$. Realistically the considered RVE is embedded within a surrounding elastic medium. Therefore we can argue that the Dirichlet problem corresponds to assuming the surrounding medium to be infinitely stiff (thus $\boldsymbol{u}^d = 0$ on $\partial\Omega$). On the other hand the Neumann problem corresponds to assuming the surrounding medium to have zero stiffness (so that $\boldsymbol{t}^d = 0$ on $\partial\Omega$). It becomes apparent that the Dirichlet and the Neumann-Eshelby solutions are two extremes, and that a general, more realistic, solution must lie in between those two extremes.

With this motivation in mind we present, in this section, an extension to the Dirichlet and Neumann result reported previously.

3.1 The general problem

We start by solving Eshelby's inclusion problem for a finite RVE with no boundary conditions prescribed. We thus seek the general solution of Somigliana's identity

$$\begin{aligned} u_m^d(\boldsymbol{x}) = &- \int_{\Omega_I} \mathbb{C}^E_{ijk\ell} G^\infty_{im,j}(\boldsymbol{x}-\boldsymbol{y}) d\Omega_y \varepsilon^*_{k\ell} + \int_{\partial\Omega} t_i^d(\boldsymbol{y}) G^\infty_{im}(\boldsymbol{x}-\boldsymbol{y}) dS_y \\ &+ \int_{\partial\Omega} \mathbb{C}^E_{ijk\ell} u_k^d(\boldsymbol{y})\, G^\infty_{im,j}(\boldsymbol{x}-\boldsymbol{y})\, n_\ell(\boldsymbol{y})\, dS_y, \quad \forall \boldsymbol{x}, \boldsymbol{y} \in \Omega, \end{aligned} \tag{3.1}$$

where neither $\boldsymbol{u}^d$ or $\boldsymbol{t}^d$ are considered zero on the boundary, so that both boundary integrals are still present.

Before deriving the general solution let us consider the convex combination of the Dirichlet and Neumann disturbance displacement fields

$$u_i^d(\boldsymbol{x}) = \alpha\, u_i^{d,D}(\boldsymbol{x}) + (1-\alpha) u_i^{d,N}(\boldsymbol{x}), \tag{3.2}$$

with $u_i^{d,D} = \mathbb{U}_{imn}^{\bullet,D}\varepsilon_{mn}^*$ and $u_i^{d,N} = \mathbb{U}_{imn}^{\bullet,N}\varepsilon_{mn}^*$ according to Box 1. It can be shown, by linear superposition, that this simple combination (3.2) satisfies. Somigliana's identity (3.1) exactly. We note that Eq. (3.2) corresponds to the combination of the displacement tensors

$$\mathbb{U}^{\bullet,C}(\boldsymbol{x}) = \alpha\, \mathbb{U}^{\bullet,D}(\boldsymbol{x}) + (1-\alpha)\, \mathbb{U}^{\bullet,N}(\boldsymbol{x}), \tag{3.3}$$

so that we can write $u_i^d = \mathbb{U}_{imn}^{\bullet,C}\varepsilon_{mn}^*$. Likewise the disturbance strain field follows as

$$\boldsymbol{\varepsilon}_{ij}^d = \mathbb{S}_{ijmn}^{\bullet,C}\varepsilon_{mn}^*, \quad \mathbb{S}^{\bullet,C}(\boldsymbol{x}) = \alpha\, \mathbb{S}^{\bullet,D}(\boldsymbol{x}) + (1-\alpha)\, \mathbb{S}^{\bullet,N}(\boldsymbol{x}). \tag{3.4}$$

Here and above the superscript C is used to denote the combination or composition of the Dirichlet and Neumann solutions. Even though (3.2) satisfies Somigliana's identity (3.1) for any α, it is not the most general result. This is derived next and we will see that further important contributions are picked up.

3.2 The general solution

Since the Finite Eshelby tensor $\mathbb{S}^{\bullet,C}$ is a combination of the Dirichlet- and Neumann-Eshelby tensor, it can also be written in decomposition (2.8) discussed in the previous section. As we have seen for the Dirichlet and the Neumann problem, this decomposition allows us to recast the integral equation (3.1) into an algebraic equation. We will therefore rewrite the three integrals appearing in (3.1) using the developments of Sect. 2.

The first integral, the domain contribution, can be written, in view of Eqs. (2.18) and (2.19), in the following two ways:

$$\begin{aligned}
\mathbf{U}^{\bullet,\infty} \cdot \boldsymbol{\Xi}_{imn}\varepsilon_{mn}^* &= -\int_{\Omega_I} \mathbb{C}_{k\ell mn} G_{ik,\ell}^{\infty}(\boldsymbol{x}-\boldsymbol{y}) d\Omega_y \varepsilon_{mn}^*, \\
\mathbf{S}^{\bullet,\infty} \cdot \boldsymbol{\Theta}_{ijmn}\varepsilon_{mn}^* &= -\frac{1}{2}\int_{\Omega_I} \Big(\mathbb{C}_{k\ell mn} G_{ik,\ell j}^{\infty}(\boldsymbol{x}-\boldsymbol{y}) + \mathbb{C}_{k\ell mn} G_{jk,\ell i}^{\infty}(\boldsymbol{x}-\boldsymbol{y}) \Big) d\Omega_y \varepsilon_{mn}^*.
\end{aligned} \tag{3.5}$$

The third integral, the Neumann boundary contribution, can be expressed by the two alternative statements

$$\mathbf{K}_N(t)\mathbf{U}^{E,C}(1) \cdot \boldsymbol{\Xi}_{imn}\varepsilon_{mn}^* = \int_{\partial\Omega} \mathbb{C}_{k\ell st} u_s^d(\boldsymbol{y}) G_{ki,\ell}^{\infty}(\boldsymbol{x}-\boldsymbol{y}) n_t(\boldsymbol{y}) dS_y, \tag{3.6.1}$$

$$[\mathfrak{D}(t)\mathbf{K}_N(t)]\mathbf{U}^{E,C}(1) \cdot \boldsymbol{\Theta}_{ijmn}\varepsilon_{mn}^* = \frac{1}{2}\int_{\partial\Omega} \mathbb{C}_{k\ell st} u_s^d(\boldsymbol{y}) \Big(G_{ki,\ell j}^{\infty} + G_{kj,\ell i}^{\infty} \Big) n_t(\boldsymbol{y}) dS_y. \tag{3.6.2}$$

Here, the equation of the displacement field, (3.6.1), follows from using Eqs. (2.31), (2.11), (2.29) and (2.33). Note that in using Eq. (2.33) superscript N is replaced by C since we are not considering the Neumann-Eshelby problem but the more general Composite Eshelby problem. The equation of the strain field, (3.6.2), follows by differentiation of (3.6.1). In view of Eq. (2.14) this means application of operator $\mathfrak{D}$. Note that the differentiation $\mathfrak{D}$ only operates on $\mathbf{K}_N(t)$ and does not affect

$\mathbf{U}^{E,C}(1), \mathbf{\Theta}_{ijmn}$ or ε^*_{mn}. Also note that the Neumann boundary contribution (3.6) is zero in the Dirichlet case ($C = D$), since $u^d_i = 0$ then.

The Dirichlet boundary contribution, i.e. the second integral in (3.1), can be written as

$$[\mathfrak{I}(t)\mathbf{K}_D(t)]\mathbf{S}^{E,C}(1) \cdot \mathbf{\Xi}_{imn}\varepsilon^*_{mn} = \int_{\partial\Omega} \mathbb{C}_{k\ell st}\, u^d_{s,t}(\boldsymbol{y}) G^\infty_{ki}(\boldsymbol{x}-\boldsymbol{y}) n_\ell(\boldsymbol{y}) dS_y, \tag{3.7.1}$$

$$\mathbf{K}_D(t)\mathbf{S}^{E,C}(1) \cdot \mathbf{\Theta}_{ijmn}\varepsilon^*_{mn} = \frac{1}{2}\int_{\partial\Omega} \mathbb{C}_{k\ell st}\varepsilon^d_{st}(\boldsymbol{y})\Big(G^\infty_{ki,j} + G^\infty_{kj,i}\Big) n_\ell(\boldsymbol{y}) dS_y. \tag{3.7.2}$$

Here (3.7.2) follows from the use of Eqs. (2.23), (2.8), (2.21) and (2.25) (now by replacing D by C), whereas (3.7.1) follows from the application of (2.16) to (3.7.2). Note that the Dirichlet boundary contribution is zero for the Neumann problem ($\boldsymbol{t}^d = 0$ on $\partial\Omega$). Further note that $\mathfrak{I}$ only operates on $\mathbf{K}_D(t)$ and does not affect $\mathbf{S}^{E,C}(1)$.

Now, Somigliana's identity (3.1), either expressed in terms of the displacement $\boldsymbol{u}^d$ or expressed in terms of the strain $\boldsymbol{\varepsilon}^d$, can be rewritten as an algebraic equation. Using the preceding Eqs. (3.5), (3.6), (3.7) and the decompositions (2.11), (2.29), (2.8), (2.21) we obtain the two coupled equations

$$\begin{aligned}
\mathbf{U}^{\bullet,C}(t) &= \mathbf{K}_N(t)\,\mathbf{U}^{E,C}(1) + [\mathfrak{I}(t)\,\mathbf{K}_D(t)]\mathbf{S}^{E,C}(1) + \mathbf{U}^{\bullet,\infty}(t),\\
\mathbf{S}^{\bullet,C}(t) &= [\mathfrak{D}(t)\,\mathbf{K}_N(t)]\;\mathbf{U}^{E,C}(1) + \mathbf{K}_D(t)\mathbf{S}^{E,C}(1) + \mathbf{S}^{\bullet,\infty}(t).
\end{aligned} \tag{3.8}$$

In particular, on the surface of the RVE ($t = 1$, $\bullet = E$), we have

$$\begin{aligned}
\mathbf{U}^{E,C}(1) &= \mathbf{K}_N(1)\mathbf{U}^{E,C}(1) + [\mathfrak{I}(t)\mathbf{K}_D(t)]_{t=1}\mathbf{S}^{E,C}(1) + \mathbf{U}^{E,\infty}(1),\\
\mathbf{S}^{E,C}(1) &= [\mathfrak{D}(t)\mathbf{K}_N(t)]_{t=1}\mathbf{U}^{E,C}(1) + \mathbf{K}_D(1)\mathbf{S}^{E,C}(1) + \mathbf{S}^{E,\infty}(1),
\end{aligned} \tag{3.9}$$

which can be written in the matrix form

$$\begin{bmatrix} \mathbf{I}_3 - \mathbf{K}_N(1) & -[\mathfrak{I}(t)\mathbf{K}_D(t)]_{t=1} \\ -[\mathfrak{D}(t)\mathbf{K}_N(t)]_{t=1} & \mathbf{I}_6 - \mathbf{K}_D(1) \end{bmatrix} \begin{bmatrix} \mathbf{U}^{E,C}(1) \\ \mathbf{S}^{E,C}(1) \end{bmatrix} = \begin{bmatrix} \mathbf{U}^{E,\infty}(1) \\ \mathbf{S}^{E,\infty}(1) \end{bmatrix}. \tag{3.10}$$

We have thus transformed the integral equation (3.1) for the unknown vectorial displacement field $\boldsymbol{u}^d$ into an algebraic equation for the unknown radial basis arrays $\mathbf{U}^{E,C}(1)$ and $\mathbf{S}^{E,C}(1)$. We remark that due to the coupling we cannot solve for the coefficients $\mathbf{U}^{E,C}(1)$ or $\mathbf{S}^{E,C}(1)$ alone. Further note that (3.10) represents the generalization of (2.28) and (2.35), which are the corresponding statements for the (decoupled) Dirichlet and Neumann special cases.

Next we derive the general solution of (3.10). Let us therefore denote the coefficient matrix by

$$\mathcal{K} = \begin{bmatrix} \mathbf{I}_3 - \mathbf{K}_N(1) & -[\mathfrak{I}(t)\,\mathbf{K}_D(t)]_{t=1} \\ -[\mathfrak{D}(t)\,\mathbf{K}_N(t)]_{t=1} & \mathbf{I}_6 - \mathbf{K}_D(1) \end{bmatrix}, \tag{3.11}$$

which is a singular matrix since the two matrix equations in (3.9) are dependent on each other: We obtain (3.9.2) by application of the derivative operator $\mathfrak{D}(t)$ to (3.9.1) and then setting $t = 1$. Vice versa (3.9.1) can be obtained by application of the integration operator $\mathfrak{I}(t)$ to (3.9.2) and then setting $t = 1$.

It is straightforward to verify that both the Dirichlet ($C = D$) and the Neumann problem ($C = N$) are solutions of (3.10), i.e.,

$$\mathcal{K}\begin{bmatrix} \mathbf{U}^{E,D}(1) \\ \mathbf{S}^{E,D}(1) \end{bmatrix} = \begin{bmatrix} \mathbf{U}^{E,\infty}(1) \\ \mathbf{S}^{E,\infty}(1) \end{bmatrix} \quad \text{and} \quad \mathcal{K}\begin{bmatrix} \mathbf{U}^{E,N}(1) \\ \mathbf{S}^{E,N}(1) \end{bmatrix} = \begin{bmatrix} \mathbf{U}^{E,\infty}(1) \\ \mathbf{S}^{E,\infty}(1) \end{bmatrix}. \tag{3.12}$$

(Note that $\mathbf{U}^{E,D}(1) = 0$ and $\mathbf{T}^{E,N}(1) = \mathbf{K}_1\,\mathbf{S}^{E,N}(1) = 0$). Furthermore, consider the arrays

$$\mathbf{U}^0(t) = \begin{bmatrix} H_0 t \\ 0 \\ 0 \end{bmatrix}, \mathbf{S}^0(t) = \begin{bmatrix} 1 \\ 0 \\ 0 \\ 0 \\ 0 \\ 0 \end{bmatrix}, \quad \mathbf{U}^{00}(t) = \begin{bmatrix} 0 \\ H_0 t \\ 0 \end{bmatrix}, \mathbf{S}^{00}(t) = \begin{bmatrix} 0 \\ 1 \\ 0 \\ 0 \\ 0 \\ 0 \end{bmatrix}, \tag{3.13}$$

where $\mathbf{U}^0$ and $\mathbf{S}^0$ as well as $\mathbf{U}^{00}$ and $\mathbf{S}^{00}$ are related by the operators $\mathfrak{D}(t)$ and $\mathfrak{I}(t)$ according to Eqs. (2.14) and (2.16). In can be easily verified that the arrays $\mathbf{U}^0$, $\mathbf{S}^0$, $\mathbf{U}^{00}$ and $\mathbf{S}^{00}$ form two zero eigenvectors (corresponding to zero eigenvalues) of $\mathcal{K}$, i.e. they satisfy

$$\mathcal{K}\begin{bmatrix} \mathbf{U}^0(1) \\ \mathbf{S}^0(1) \end{bmatrix} = \begin{bmatrix} 0 \\ 0 \end{bmatrix}, \quad \mathcal{K}\begin{bmatrix} \mathbf{U}^{00}(1) \\ \mathbf{S}^{00}(1) \end{bmatrix} = \begin{bmatrix} 0 \\ 0 \end{bmatrix}. \tag{3.14}$$

In view of (3.12) and (3.14) we thus have the three zero eigenvectors

$$\begin{bmatrix} \mathbf{U}^{E,D}(1) \\ \mathbf{S}^{E,D}(1) \end{bmatrix} - \begin{bmatrix} \mathbf{U}^{E,N}(1) \\ \mathbf{S}^{E,N}(1) \end{bmatrix}, \quad \begin{bmatrix} \mathbf{U}^{0}(1) \\ \mathbf{S}^{0}(1) \end{bmatrix}, \quad \begin{bmatrix} \mathbf{U}^{00}(1) \\ \mathbf{S}^{00}(1) \end{bmatrix}. \tag{3.15}$$

Therefore the rank of $\mathcal{K}$ can be at most 6, i.e. rank $(\mathcal{K}) \leq 6$. On the other hand we know that the submatrix $\mathbf{I}_6 - \mathbf{K}_D(1)$ is invertible, therefore the rank of $\mathcal{K}$ is at least 6 $(\text{rank}(\mathcal{K}) \geq 6)$. So we conclude that $\text{rank}(\mathcal{K}) = 6$ and that therefore the complete solution of (3.10) can only be the combination

$$\begin{aligned} \mathbf{U}^{E,C}(1) &= \alpha \mathbf{U}^{E,D}(1) + (1-\alpha)\mathbf{U}^{E,N}(1) + \beta \mathbf{U}^0(1) + \gamma\ \mathbf{U}^{00}(1), \\ \mathbf{S}^{E,C}(1) &= \alpha\ \mathbf{S}^{E,D}(1) + (1-\alpha)\mathbf{S}^{E,N}(1) + \beta\ \mathbf{S}^0(1) + \gamma \mathbf{S}^{00}(1), \end{aligned} \tag{3.16}$$

$\forall\ \alpha, \beta, \gamma$. (Note that $\mathbf{U}^{E,D}(1) = 0$.) Plugging Eqs. (3.16) into (3.8) we arrive at

$$\begin{aligned} \mathbf{U}^{\bullet,C}(t) &= \alpha \mathbf{U}^{\bullet,D}(t) + (1-\alpha)\mathbf{U}^{\bullet,N}(t) + \beta \mathbf{U}^0(t) + \gamma \mathbf{U}^{00}(t), \\ \mathbf{S}^{\bullet,C}(t) &= \alpha \mathbf{S}^{\bullet,D}(t) + (1-\alpha)\mathbf{S}^{\bullet,N}(t) + \beta \mathbf{S}^0(t) + \gamma \mathbf{S}^{00}(t), \end{aligned} \tag{3.17}$$

which is the equation for the radial basis arrays $\mathbf{U}^{\bullet,C}$ and $\mathbf{S}^{\bullet,C}$ of the Composite Eshelby tensors $\mathbb{U}^{\bullet,C}$ and $\mathbb{S}^{\bullet,C}$ which solve Somigliana's identity (3.1) exactly. Note that the two Eqs. (3.17.1) and (3.17.2) depend on each other via $\mathfrak{D}(t)$ and $\mathfrak{I}(t)$. Using the definition of $\mathbf{U}^{\bullet,D}$, $\mathbf{U}^{\bullet,N}$, $\mathbf{S}^{\bullet,D}$ and $\mathbf{S}^{\bullet,N}$ (from Box 1 and 2), Eq. (3.17) can equivalently be written as

$$\begin{aligned} \mathbf{U}^{\bullet,C}(t) &= \mathbf{U}^{\bullet,\infty}(t) + \alpha \mathbf{U}^{B,D}(t) + (1-\alpha)\mathbf{U}^{B,N}(t) + \beta \mathbf{U}^0(t) + \gamma\, \mathbf{U}^{00}(t), \\ \mathbf{S}^{\bullet,C}(t) &= \mathbf{S}^{\bullet,\infty}(t) + \alpha \mathbf{S}^{B,D}(t) + (1-\alpha)\mathbf{S}^{B,N}(t) + \beta \mathbf{S}^0(t) + \gamma \mathbf{S}^{00}(t). \end{aligned} \tag{3.18}$$

Here, all the individual contributions to $\mathbf{U}^{\bullet,C}$ and $\mathbf{S}^{\bullet,C}$, for both $\bullet = I,E$, are given in Appendix A. We finally remark that the traction basis corresponding to the zero eigenvectors $\mathbf{U}^0$ and $\mathbf{U}^{00}$ is

$$\mathbf{T}^0(t) = \mathbf{K}_1 \mathbf{S}^0(t) = \begin{bmatrix} 3\kappa \\ 0 \\ 0 \end{bmatrix}, \quad \mathbf{T}^{00}(t) = \mathbf{K}_1 \mathbf{S}^{00}(t) = \begin{bmatrix} 2\lambda \\ 2\mu \\ 0 \end{bmatrix}. \tag{3.19}$$

where $\lambda = \kappa - \frac{2}{3}\mu$. Thus $\mathbf{T}^0$ and $\mathbf{U}^0$ are associated with a pure volumetric deformation, while $\mathbf{T}^{00} - \frac{2}{3}\mathbf{T}^0$ and $\mathbf{U}^{00} - \frac{2}{3}\mathbf{U}^0$ are associated with a pure deviatoric deformation. A summary of the Composite Eshelby tensors is given in Box 3.

Box 3. Composite Eshelby tensors

Disturbance displacement, strain and traction fields (• = I, E)

$$u_i^d = \mathbb{U}_{imn}^{\bullet,C}\varepsilon_{mn}^* \qquad \varepsilon_{ij}^d = \mathbb{S}_{ijmn}^{\bullet,C}\varepsilon_{mn}^*, \qquad t_i^d = \mathbb{T}_{imn}^{\bullet,C}\varepsilon_{mn}^*.$$

Radial and circumference basis decomposition

$$\mathbb{U}_{imn}^{\bullet,C}(\boldsymbol{x}) = \mathbf{U}^{\bullet,C}(t)\cdot\boldsymbol{\Xi}_{imn}(\boldsymbol{r}), \quad \boldsymbol{\Xi}_{imn}(\boldsymbol{r}) \text{ from (2.12)},$$
$$\mathbb{S}_{ijmn}^{\bullet,C}(\boldsymbol{x}) = \mathbf{S}^{\bullet,C}(t)\cdot\boldsymbol{\Theta}_{ijmn}(\boldsymbol{r}), \quad \boldsymbol{\Theta}_{ijmn}(\boldsymbol{r}) \text{ from (2.9)},$$
$$\mathbb{T}_{imn}^{\bullet,C}(\boldsymbol{x}) = \mathbf{T}^{\bullet,C}(t)\cdot\boldsymbol{\Xi}_{imn}(\boldsymbol{r}).$$

Radial basis equations

$$\mathbf{U}^{\bullet,C}(t) = \alpha\mathbf{U}^{\bullet,D}(t) + (1-\alpha)\mathbf{U}^{\bullet,\mathrm{N}}(\mathrm{t}) + \beta\mathbf{U}^{0}(\mathrm{t}) + \gamma\ \mathbf{U}^{00}(\mathrm{t}),$$
$$\mathbf{S}^{\bullet,C}(t) = \alpha\mathbf{S}^{\bullet,D}(t) + (1-\alpha)\mathbf{S}^{\bullet,\mathrm{N}}(\mathrm{t}) + \beta\mathbf{S}^{0}(\mathrm{t}) + \gamma\ \mathbf{S}^{00}(\mathrm{t}),$$
$$\mathbf{T}^{\bullet,C}(t) = \alpha\mathbf{T}^{\bullet,D}(t) + (1-\alpha)\mathbf{T}^{\bullet,\mathrm{N}}(\mathrm{t}) + \beta\ \mathbf{T}^{0}(\mathrm{t}) + \gamma\mathbf{T}^{00}(\mathrm{t}).$$

See Box 1, Box 2, Eqs, (2.40), (3.13) and (3.19) for individual contributions

3.3 The physical solution

To satisfy Somigliana's identity (3.1) by solution (3.17), α, β and γ can be arbitrary. However not any choice will make physical sense. Next we derive physical meaningful values of these parameters. The derivation is based on the work by Luo and Weng [19]. Their idea is to consider the two-phase RVE to be embedded within the surrounding homogenized composite Ω_c, an isotropic elastic medium with stiffness κ_c and μ_c, and Poisson's ratio v_c, as shown in Fig. 2. This assumption will provide us with physical conditions at the interface between composite and RVE from which α, β and γ can be solved.

We begin by studying the case of a deviatoric deformation. Adopting the spherical coordinates $\{r,\ \varphi,\ \theta\}$, as displayed in Fig. 2, it has been shown by [2] that the displacement field can be expressed as

$$\begin{aligned} u_r &= U_r(r)\sin^2\theta\cos 2\varphi, \\ u_\theta &= U_\theta(r)\sin\theta\cos\theta\cos 2\varphi, \\ u_\varphi &= U_\varphi(r)\sin\theta\sin 2\varphi, \end{aligned} \tag{3.20}$$

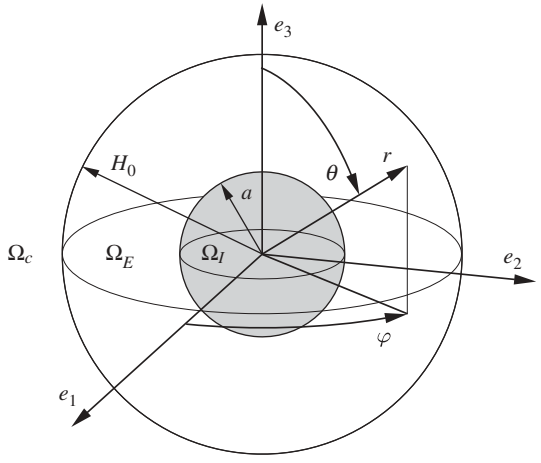

Fig. 2. RVE embedded within a surrounding Composite Ω_c

where U_r, U_φ and U_θ are functions of the radial coordinate r. For the disturbance displacement field of the composite surrounding the RVE region, $\boldsymbol{u}_c^d$, these are

$$\begin{aligned} U_r^c(r) &= \frac{3C_3}{r^4} + \frac{5-4\nu_c}{1-2\nu_c}\frac{C_4}{r^2}, \\ U_\varphi^c(r) &= \frac{3C_3}{r^4} - \frac{2C_4}{r^2} = -U_\theta^c(r), \end{aligned} \tag{3.21}$$

where C_3 and C_4 are unknown constants to be determined. Employing the strain displacement relation (2.13) and the constitutive relation $\boldsymbol{\sigma} = \mathbb{C}^c : \boldsymbol{\varepsilon}$, where $\mathbb{C}^c$ is the isotropic elasticity tensor of the composite, the stress components acting on the surface of a sphere centered at the origin follow as

$$\begin{aligned} \sigma_{rr}^c &= -\left[4\mu_c\left[\frac{6C_3}{r^5} + \frac{5-4\nu_c}{1-2\nu_c}\frac{C_4}{r^3}\right] + \lambda_c\frac{6C_4}{r^3}\right]\sin^2\theta\cos 2\varphi, \\ \sigma_{r\varphi}^c &= -4\mu_c\left[\frac{4C_3}{r^5} + \frac{1+\nu_c}{1-2\nu_c}\frac{C_4}{r^3}\right]\sin\theta\sin 2\varphi, \\ \sigma_{r\theta}^c &= 4\mu_c\left[\frac{4C_3}{r^5} + \frac{1+\nu_c}{1-2\nu_c}\frac{C_4}{r^3}\right]\sin\theta\cos\theta\cos 2\varphi, \end{aligned} \tag{3.22}$$

where μ_c and ν_c are the shear modulus and Poisson's ratio of the surrounding composite. The disturbance displacement field is in a state of shear when we consider the prescribed eigenstrain contribution

$$\boldsymbol{\varepsilon}^* = (\boldsymbol{e}_1 \otimes \boldsymbol{e}_1 - \boldsymbol{e}_2 \otimes \boldsymbol{e}_2)e^*, \tag{3.23}$$

where e^* is some constant. We note that this corresponds to shearing of the $\boldsymbol{e}_1$, $\boldsymbol{e}_2$ plane, the consideration of which suffices for our needs. For this eigenstrain $\boldsymbol{\varepsilon}^*$ the disturbance displacement field, given in Box 3 and evaluated at the boundary of the RVE ($t = 1$), follows in spherical coordinates as

$$\begin{aligned} u_r^d(\boldsymbol{y}) &= \Big[(1-\alpha)\Big[2U_2^{E,N}(1) + U_3^{E,N}(1)\Big] + 2\gamma U_2^{00}(1)\Big]\sin^2\theta\cos 2\varphi\; e^*, \\ u_\varphi^d(\boldsymbol{y}) &= -2\Big[(1-\alpha)U_2^{E,N}(1) + \gamma U_2^{00}(1)\Big]\sin\theta\sin 2\varphi\; e^*, \\ u_\theta^d(\boldsymbol{y}) &= -u_\varphi^d(\boldsymbol{y})\cos\theta\cot 2\varphi, \end{aligned} \tag{3.24}$$

which does not depend on the Dirichlet-Eshelby coefficients $\mathbf{U}^{E,D}$ since $\mathbf{U}^{E,D}(1) = \mathbf{0}$. Likewise, for the prescribed eigenstrain (3.23), the disturbance traction field (see Box 3) on the RVE surface becomes

$$\begin{aligned} t_r^d(\boldsymbol{y}) &= \Big[\alpha\Big[2T_2^{E,D}(1) + T_3^{E,D}(1)\Big] + 2\gamma\; T_2^{00}(1)\Big]\sin^2\theta\cos 2\varphi\; e^*, \\ t_\varphi^d(\boldsymbol{y}) &= -2\Big[\alpha T_2^{E,D}(1) + \gamma T_2^{00}(1)\Big]\sin\theta\sin 2\varphi\; e^*, \\ t_\theta^d(\boldsymbol{y}) &= -t_\varphi^d(\boldsymbol{y})\cos\theta\cot 2\varphi, \end{aligned} \tag{3.25}$$

which does not depend on the Neumann-Eshelby coefficients $\mathbf{T}^{E,N}$ since $\mathbf{T}^{E,N}(1) = \mathbf{0}$. Also note that both (3.24) and (3.25) are independent of β. At the interface between RVE and surrounding composite, where $r = H_0$, we require the continuity of the displacement field

$$\begin{aligned} u_r^d(\boldsymbol{y}) &= u_r^c(H_0), \\ u_\theta^d(\boldsymbol{y}) &= u_\theta^c(H_0), \end{aligned} \tag{3.26}$$

and the continuity of the traction field

$$\begin{aligned} t_r^d(\boldsymbol{y}) &= \sigma_{rr}^c(H_0), \\ t_\theta^d(\boldsymbol{y}) &= \sigma_{r\theta}^c(H_0). \end{aligned} \tag{3.27}$$

Note that the conditions on u_θ and t_θ are mathematically equivalent to the conditions on u_φ and t_φ and have therefore been omitted. Equations (3.26) and (3.27) give four expressions for the 4 unknowns α, γ, C_3 and C_4. These can be solved for α and γ, giving

$$\alpha = \frac{4\mu_c(7-10\nu)}{4\mu_c(7-10\nu)+\mu(7+5\nu)}, \tag{3.28}$$

and

$$\gamma = \frac{f}{2}(\alpha-\bar{\gamma}), \quad \bar{\gamma} = \frac{\mu_c(7-5\nu_c)}{\mu_c(7-5\nu_c)+2\mu(4-5\nu_c)}. \tag{3.29}$$

We note that γ depends on both the bulk modulus κ_c (via ν_c) and the shear modulus μ_c of the composite whereas α only depends on μ_c. Physically, the surrounding composite must satisfy $0 < \mu_c < \infty$. We can see from Eq. (3.28) that this leads to the restriction $0 < \alpha < 1$. The limit case $\mu_c = \infty$, implying $\alpha = 1$ and $\gamma = 0$, corresponds to the Dirichlet problem as discussed earlier. Conversely the limit $\mu_c = 0$ implies $\alpha = 0$ and $\gamma = 0$, which corresponds to the Neumann problem.

To obtain β we need to consider hydrostatic deformation. For this radially symmetric case the only nonzero displacement component is [2]

$$u_r = C_1 r + \frac{C_2}{r^2}, \tag{3.30}$$

for some constants C_1 and C_2. In the surrounding composite the disturbance field due to the inclusion must decay so that $C_1 = 0$ and we can write

$$u_r^c = \frac{C_2}{r^2}. \tag{3.31}$$

For a linear elastic isotropic composite the stress in radial direction then becomes

$$\sigma_{rr}^c = -6\kappa_c \frac{C_2}{r^3}. \tag{3.32}$$

The hydrostatic eigenstrains can be expressed as $\varepsilon_{ij}^* = \varepsilon^* \delta_{ij}$, for some constant ε^*. Thus the radial components of the disturbance fields, $u_r^d = \boldsymbol{u}^d \cdot \boldsymbol{e}_r$ and $t_r^d = \boldsymbol{t}^d \cdot \boldsymbol{e}_r$, follow from Box 3 as

$$\begin{aligned} u_r^d(\boldsymbol{y}) &= \Big[(1-\alpha)\Big[3\,U_1^{E,N}(1) + 2\,U_2^{E,N} + U_3^{E,N}(1)\Big] + 3\beta H_0 + 2\gamma H_0\Big]\varepsilon^*, \\ t_r^d(\boldsymbol{y}) &= \Big[\alpha\Big[3\,T_1^{E,D}(1) + 2\,T_2^{E,D} + T_3^{E,D}(1)\Big] + 3\beta\, T_1^0(1) + \gamma\big[3\,T_1^{00}(1) + 2\,T_2^{00}(1)\big]\Big]\varepsilon^*. \end{aligned} \tag{3.33}$$

As for the shear case, we impose the continuity conditions

$$u_r^d(\boldsymbol{y}) = u_r^c(H_0), \tag{3.34.1}$$

$$t_r^d(\boldsymbol{y}) = \sigma_{rr}^c(H_0)\,, \tag{3.34.2}$$

at the interface between the RVE and composite. This provides two equations for the final two unknowns β and C_2. For β we find

$$\beta = \frac{f}{3}(\bar{\gamma}-\bar{\beta})\,, \quad \bar{\beta} = \frac{4\mu_c(1-2\nu)}{4\mu_c(1-2\nu)+2\mu(1+\nu)}\,. \tag{3.35}$$

With the specified values of α, β and γ the Composite Eshelby tensors $\mathbb{U}^{\bullet,C}(\boldsymbol{x})$ and $\mathbb{S}^{\bullet,C}(\boldsymbol{x})$ are completely determined by the expressions in Box 3 and Appendix A. Note that these tensors depend on the volume fraction f, the comparison solid (μ, κ) and the composite solid (μ_c, κ_c). As a concluding statement of the preceding derivation, let us remark that the Composite Eshelby tensors $\mathbb{U}^{\bullet,C}$ and $\mathbb{S}^{\bullet,C}$ satisfy Somigliana's identity exactly for any volume fraction f and coefficients α, β, γ. For the particular α, β and γ above we furthermore satisfy the continuity of all elastic fields at the interface of RVE and surrounding composite.

Similar to the limits of γ we obtain $\beta = 0$ for both the Dirichlet case ($\mu_c = \infty$) and the Neumann case ($\mu_c = 0$). The fact that β and γ are zero for the Dirichlet and Neumann special cases is very important, because it shows (from Eq. (3.17)) that the Dirichlet- and Neumann-Eshelby results are special cases of the Composite Eshelby tensor. Another special case is $\mu_c = \mu$ and $\nu_c = \nu$, which corresponds to considering the composite and the comparison solid to have the same properties. Computing the particular values of α, β and γ it can be shown from (3.18) that this case will give us the original infinite Eshelby Tensor $\mathbb{S}^{\bullet,\infty}$. The three special cases discussed above can be summarized as follows:

$$\begin{aligned}
&\mathbf{S}^{\bullet,C}(t) = \mathbf{S}^{\bullet,D}(t) \quad \text{for } \mu_c = \infty\,,\\
&\mathbf{S}^{\bullet,C}(t) = \mathbf{S}^{\bullet,\infty}(t) \quad \text{for } \mu_c = \mu\,,\\
&\mathbf{S}^{\bullet,C}(t) = \mathbf{S}^{\bullet,N}(t) \quad \text{for } \mu_c = 0\,.
\end{aligned} \tag{3.36}$$

Figure 3 shows a plot of the coefficients of the displacement Eshelby tensor $\mathbf{U}^C$ for shear modulus $\mu_c/\mu = \{0, \frac{1}{3}, 1, 3, \infty\}$ and inclusion ratio $\rho_0 = 0.4$. Poisson's ratio of both the matrix (the comparison phase) and the composite is chosen as $\nu = \nu_c = 0.3$. According to Eq. (3.36), which holds analogously for $\mathbf{U}^{\bullet,C}$, $\mu_c = \infty$, $\mu_c = \mu$ and $\mu_c = 0$ correspond to the Dirichlet-, the original

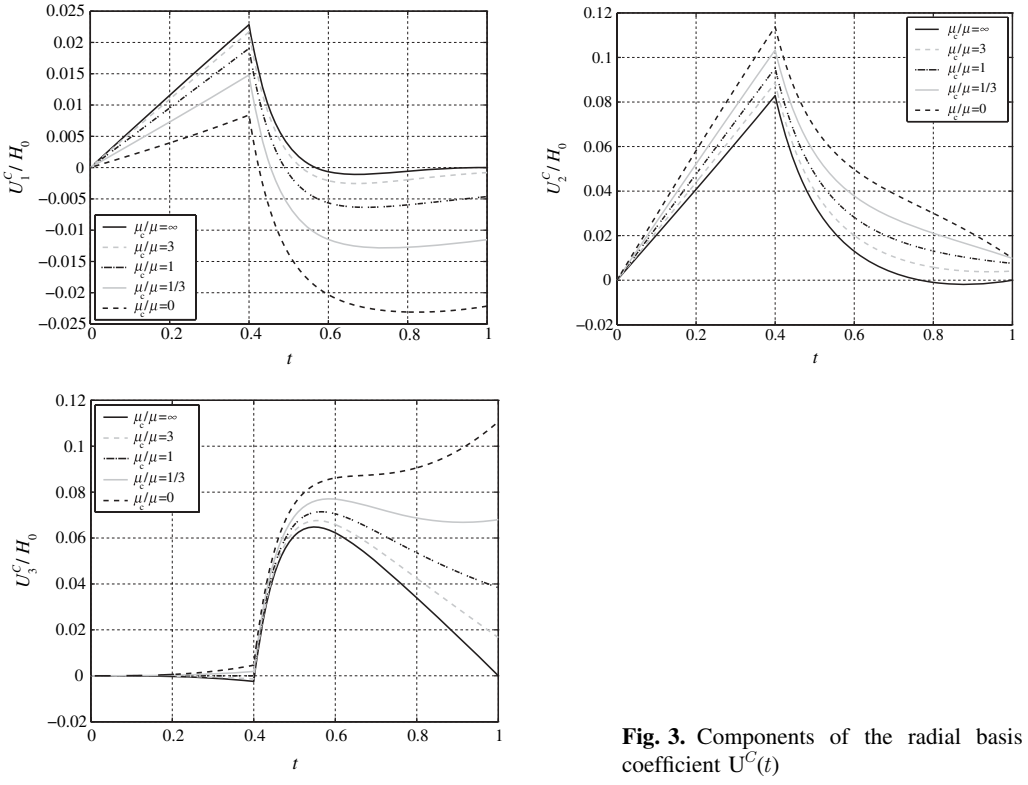

Fig. 3. Components of the radial basis coefficient $\mathrm{U}^C(t)$

infinite and the Neumann-Eshelby problem. We observe that the components of $\mathbf{U}^C(t)$ are continuous functions of t with a kink at the material interface $t = \rho_0$. They vary smoothly with μ_c. Note that for composite moduli μ_c differing significantly from μ the Composite Eshelby tensor will differ significantly from the original Eshelby tensor. This is despite the fact that the volume fraction is small, i.e. $f = \rho_0^3 = 0.064$.

We remark that since the strain and traction bases $\mathbf{S}^{\bullet,C}$ and $\mathbf{T}^{\bullet,C}$ are related to $\mathbf{U}^{\bullet,C}$ (by (2.14) and (2.39)), the behavior of both $\mathbf{S}^{\bullet,C}$ and $\mathbf{T}^{\bullet,C}$ will be similar to the behavior of $\mathbf{U}^{\bullet,C}$, shown in Fig. 3.

3.4 The average solution

We finally discuss the spatial average of the Composite Eshelby tensor. As we have shown in [16] the domain average of $\mathbb{S}^{I,C}$ over the interior domain Ω_I and the average of $\mathbb{S}^{E,C}$ over the exterior domain Ω_E can be written as

$$\begin{aligned}\langle \mathbb{S}^{I,C}_{ijmn}\rangle_{\Omega_I} &= s_1^{I,C}\mathbb{E}^{(1)}_{ijmn} + s_2^{I,C}\mathbb{E}^{(2)}_{ijmn}\,,\\ \langle \mathbb{S}^{E,C}_{ijmn}\rangle_{\Omega_E} &= s_1^{E,C}\,\mathbb{E}^{(1)}_{ijmn} + s_2^{E,C}\,\mathbb{E}^{(2)}_{ijmn}\,,\end{aligned} \tag{3.37}$$

where $\mathbb{E}^{(1)}_{ijmn}$ and $\mathbb{E}^{(2)}_{ijmn}$ are the isotropic basis tensors

$$\mathbb{E}^{(1)}_{ijmn} = \frac{1}{3}\delta_{ij}\delta_{mn}\,, \quad \mathbb{E}^{(2)}_{ijmn} = \frac{1}{2}(\delta_{im}\delta_{jn} + \delta_{in}\delta_{jm}) - \frac{1}{3}\delta_{ij}\delta_{mn}\,. \tag{3.38}$$

The coefficients $s_1^{I,C}$, $s_2^{I,C}$ and $s_1^{E,C}$, $s_2^{E,C}$ are related to the radial basis $\mathbf{S}^{I,C}$ and $\mathbf{S}^{E,C}$ by

$$\begin{aligned}\begin{bmatrix} s_1^{I,C}\\ s_2^{I,C}\end{bmatrix} &= \begin{bmatrix} 3 & 2 & 1 & 1 & \frac{4}{3} & \frac{1}{3}\\ 0 & 2 & 0 & 0 & \frac{4}{3} & \frac{2}{15}\end{bmatrix}\langle 3t^2\mathbf{S}^{I,C}\rangle_{[0,\rho_0]}\,,\\ \begin{bmatrix} s_1^{E,C}\\ s_2^{E,C}\end{bmatrix} &= \begin{bmatrix} 3 & 2 & 1 & 1 & \frac{4}{3} & \frac{1}{3}\\ 0 & 2 & 0 & 0 & \frac{4}{3} & \frac{2}{15}\end{bmatrix}\langle 3t^2\mathbf{S}^{E,C}\rangle_{[\rho_0,1]}\end{aligned} \tag{3.39}$$

with

$$\langle \ldots\rangle_{[a,b]} := \frac{1}{b^3-a^3}\int_a^b \ldots dt. \tag{3.40}$$

Due to Eq. (3.17) we can immediately write

$$s_i^{\bullet,C} = \alpha s_i^{\bullet,D} + (1-\alpha)s_i^{\bullet,N} + \beta s_i^0 + \gamma\; s_i^{00}\,, \tag{3.41}$$

for $i = 1, 2$ and $\bullet = I, E$. The individual pieces are all given in Appendix A. We will see that an important object is the difference

$$\langle \mathbb{S}^{I,C}_{ijmn}\rangle_{\Omega_I} - \langle \mathbb{S}^{E,C}_{ijmn}\rangle_{\Omega_E} = \Delta s_1^C\,\mathbb{E}^{(1)}_{ijmn} + \Delta s_2^C\mathbb{E}^{(2)}_{ijmn}\,, \tag{3.42}$$

where we have defined

$$\Delta s_i^C := s_i^{I,C} - s_i^{E,C} = \alpha\Delta s_i^D + (1-\alpha)\Delta s_i^N. \tag{3.43}$$

The coefficients $\Delta s_i^D := s_i^{I,D} - s_i^{E,D}, \Delta s_i^N := s_i^{I,N} - s_i^{E,N}$ and Δs_i^C are also given in Appendix A for the α reported in Eq. (3.28).

4 The dual eigenstrain method

In this section we illustrate how the Composite Eshelby tensor affects the computation of the effective elastic modulus $\overline{\mathbb{C}}$. Therefore we introduce a general homogenization method termed the 'Dual Eigenstrain Method', which, as we will see, contains the classical dilute distribution, Mori-Tanaka and self-consistent homogenization methods while further defining some entirely new methods.

4.1 The dual eigenstrain homogenization

Consider a two phase composite solid with phase moduli $\mathbb{C}^I$ and $\mathbb{C}^E$. The phases are arranged concentrically in regions Ω_I and Ω_E as illustrated in Fig. 4. The idea of the dual eigenstrain method is to prescribe an eigenstrain in both the inclusion and matrix phase as

$$\boldsymbol{\varepsilon}^*(\boldsymbol{x}) = \begin{cases} \boldsymbol{\varepsilon}_I^*\,, & \boldsymbol{x} \in \Omega_I\,, \\ \boldsymbol{\varepsilon}_E^*\,, & \boldsymbol{x} \in \Omega_E\,. \end{cases} \tag{4.1}$$

As before we focus on constants $\boldsymbol{\varepsilon}_I^*$ and $\boldsymbol{\varepsilon}_E^*$. This formulation admits the two special cases $\boldsymbol{\varepsilon}_E^* = 0$ and $\boldsymbol{\varepsilon}_I^* = 0$ as shown in Fig. 4: In the interior eigenstrain approach, where $\boldsymbol{\varepsilon}_E^* = 0, \boldsymbol{\varepsilon}_I^*$ is introduced to account for the misfit in the material response arising from setting $\mathbb{C}^E$ as the stiffness of both phases. Likewise, in the exterior eigenstrain approach, where $\boldsymbol{\varepsilon}_I^* = 0, \boldsymbol{\varepsilon}_E^*$ accounts for letting $\mathbb{C}^I$ be the comparison stiffness. As we prescribe non-zero $\boldsymbol{\varepsilon}_I^*$ and $\boldsymbol{\varepsilon}_E^*$ the comparison solid can neither have stiffness $\mathbb{C}^I$ nor $\mathbb{C}^E$. We thus introduce the elasticity tensor $\widetilde{\mathbb{C}}$ to characterize the comparison solid of the two phases within the framework of the dual eigenstrain method. In taking such a homogenization approach the average stress consistency condition becomes

$$\begin{aligned} \mathbb{C}^I : (\boldsymbol{\varepsilon}^0 + \langle \boldsymbol{\varepsilon}^d \rangle_{\Omega_I}) &= \widetilde{\mathbb{C}} : (\boldsymbol{\varepsilon}^0 + \langle \boldsymbol{\varepsilon}^d \rangle_{\Omega_I} - \boldsymbol{\varepsilon}_I^*)\,, \qquad \boldsymbol{x} \in \Omega_I\,, \\ \mathbb{C}^E : (\boldsymbol{\varepsilon}^0 + \langle \boldsymbol{\varepsilon}^d \rangle_{\Omega_E}) &= \widetilde{\mathbb{C}} : (\boldsymbol{\varepsilon}^0 + \langle \boldsymbol{\varepsilon}^d \rangle_{\Omega_E} - \boldsymbol{\varepsilon}_E^*)\,, \qquad \boldsymbol{x} \in \Omega_E\,. \end{aligned} \tag{4.2}$$

We remark that from $\boldsymbol{\varepsilon}_E^* = 0$ follows $\widetilde{\mathbb{C}} = \mathbb{C}^E$ and that $\boldsymbol{\varepsilon}_I^* = 0$ implies $\widetilde{\mathbb{C}} = \mathbb{C}^I$. The Eshelby tensor following from Eq. (4.2) depends on $\widetilde{\mathbb{C}}$, the modulus of the homogenized comparison solid. Since we

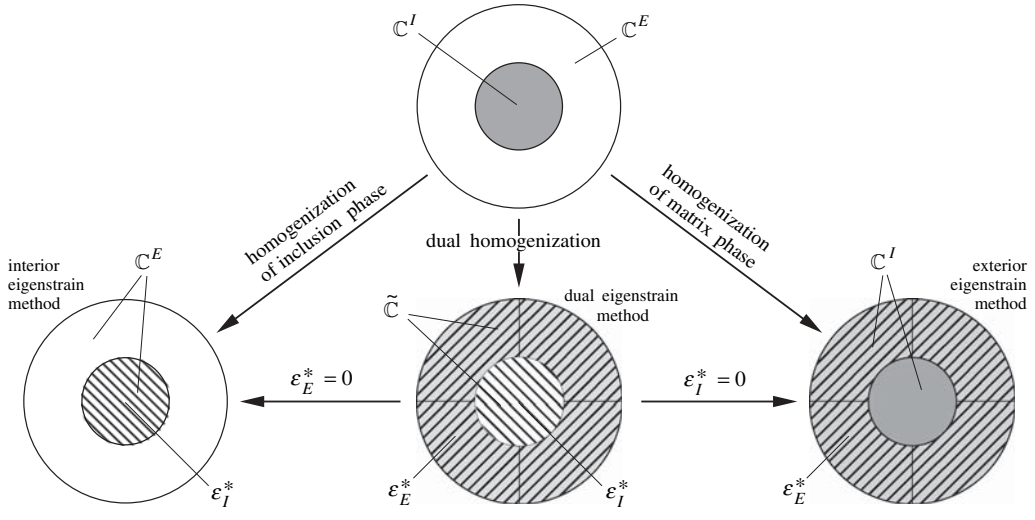

Fig. 4. Dual eigenstrain homogenization

are prescribing two eigenstrain fields $\boldsymbol{\varepsilon}_I^*$ and $\boldsymbol{\varepsilon}_E^*$ we have two Eshelby tensors. The first, $\mathbb{S}^{\bullet,C}$, gives the disturbance strain field $\boldsymbol{\varepsilon}_I^d$ caused by the interior eigenstrain $\boldsymbol{\varepsilon}_I^*$. The second, $\overline{\mathbb{S}}^{\bullet,C}$, relates the disturbance field $\boldsymbol{\varepsilon}_E^d$ to the exterior eigenstrain $\boldsymbol{\varepsilon}_E^*$. Therefore the total disturbance strain field is written as

$$\begin{aligned}
\boldsymbol{\varepsilon}^d(\boldsymbol{x}) &= \boldsymbol{\varepsilon}_I^d(\boldsymbol{x}) + \boldsymbol{\varepsilon}_E^d(\boldsymbol{x}),\\
\boldsymbol{\varepsilon}_I^d(\boldsymbol{x}) &= \mathbb{S}^{\bullet,C}(\boldsymbol{x}) : \boldsymbol{\varepsilon}_I^*,\\
\boldsymbol{\varepsilon}_E^d(\boldsymbol{x}) &= \overline{\mathbb{S}}^{\bullet,C}(\boldsymbol{x}) : \boldsymbol{\varepsilon}_E^*.
\end{aligned} \tag{4.3}$$

Note that both $\boldsymbol{\varepsilon}_I^d$ and $\boldsymbol{\varepsilon}_E^d$ are given for all $\boldsymbol{x} \in \Omega$ through the use of the interior Eshelby tensor ($\bullet = I$ for $\boldsymbol{x} \in \Omega_I$) and exterior Eshelby tensor ($\bullet = E$ for $\boldsymbol{x} \in \Omega_E$). $\mathbb{S}^{\bullet,C}$ has been derived earlier (see Box 3 and Appendix A). The simple illustration of Fig. 5 shows that $\overline{\mathbb{S}}_E^{\bullet,C}$ can be written as

$$\overline{\mathbb{S}}^{\bullet,C}(\boldsymbol{x}) = \mathbb{S}^{I,C}(\boldsymbol{x})\big|_{f=1} - \mathbb{S}^{\bullet,C}(\boldsymbol{x}). \tag{4.4}$$

Let us emphasize that the material constants appearing in $\mathbb{S}^{\bullet,C}$ are those of the comparison solid, i.e. $\nu = \tilde{\nu}$ and $\mu = \tilde{\mu}$. Further note that $\mathbb{S}^{\bullet,C}$ depends on the volume fraction of the interior phase, i.e. $f = f_I$, and that we can write $f_E = 1 - f_I$. The validity of Eqs. (4.3) and (4.4) can be proved by showing that they satisfy Somigliana's identity (2.3) exactly. We note that the superposition procedure displayed in Fig. 5 can also be used for n nested shells. Such a shell model has been investigated in [16].

4.2 The effective modulus

With the above relation we can now derive the effective modulus of the dual eigenstrain method. We start by defining the concentration tensors $\mathbb{A}_I$ and $\mathbb{A}_E$ and rewrite the average stress consistency condition as

$$\begin{aligned}
\boldsymbol{\varepsilon}^0 + \langle \boldsymbol{\varepsilon}^d \rangle_{\Omega_I} &= \mathbb{A}_I : \boldsymbol{\varepsilon}_I^*, \qquad \boldsymbol{x} \in \Omega_I, \quad \mathbb{A}_I := \left[\widetilde{\mathbb{C}} - \mathbb{C}^I\right]^{-1} : \widetilde{\mathbb{C}},\\
\boldsymbol{\varepsilon}^0 + \langle \boldsymbol{\varepsilon}^d \rangle_{\Omega_E} &= \mathbb{A}_E : \boldsymbol{\varepsilon}_E^*, \qquad \boldsymbol{x} \in \Omega_E, \quad \mathbb{A}_E := \left[\widetilde{\mathbb{C}} - \mathbb{C}^E\right]^{-1} : \widetilde{\mathbb{C}}.
\end{aligned} \tag{4.5}$$

We note that $\mathbb{A}_I$ and $\mathbb{A}_E$ are ill-defined for the cases $\widetilde{\mathbb{C}} = \mathbb{C}^I$ and $\widetilde{\mathbb{C}} = \mathbb{C}^E$. To avoid this problem the following derivation can alternatively be written using only $\mathbb{A}_I^{-1}$ and $\mathbb{A}_E^{-1}$. This, however, comes at the expense of clarity.

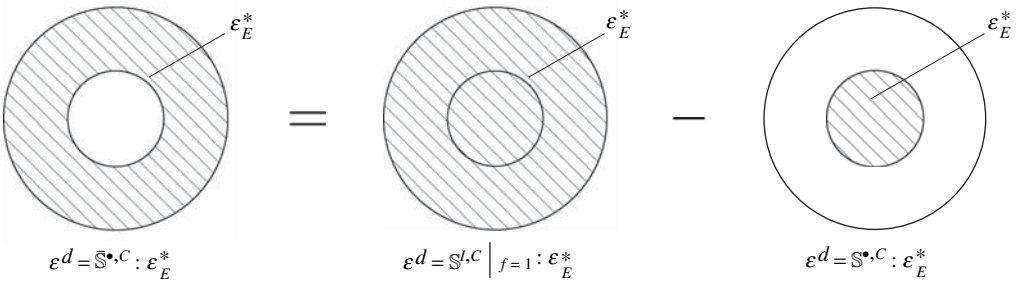

Fig. 5. Superposition of the exterior eigenstrain

The average disturbance strain in the two phases follows from (4.3) as

$$\begin{aligned}\langle\boldsymbol{\varepsilon}^d\rangle_{\Omega_I} &= \langle\mathbb{S}^{I,C}\rangle_{\Omega_I} : \boldsymbol{\varepsilon}_I^* + \langle\overline{\mathbb{S}}^{I,C}\rangle_{\Omega_I} : \boldsymbol{\varepsilon}_E^*\,,\\ \langle\boldsymbol{\varepsilon}^d\rangle_{\Omega_E} &= \langle\mathbb{S}^{E,C}\rangle_{\Omega_E} : \boldsymbol{\varepsilon}_I^* + \langle\overline{\mathbb{S}}^{E,C}\rangle_{\Omega_E} : \boldsymbol{\varepsilon}_E^*\,.\end{aligned} \tag{4.6}$$

Substituting these two expression into (4.5) yields the system of linear equations

$$\begin{bmatrix} \mathbb{A}_I - \langle\mathbb{S}^{I,C}\rangle_{\Omega_I} & -\langle\overline{\mathbb{S}}^{I,C}\rangle_{\Omega_I} \\ -\langle\mathbb{S}^{E,C}\rangle_{\Omega_E} & \mathbb{A}_E - \langle\overline{\mathbb{S}}^{E,C}\rangle_{\Omega_E} \end{bmatrix} : \begin{bmatrix} \boldsymbol{\varepsilon}_I^* \\ \boldsymbol{\varepsilon}_E^* \end{bmatrix} = \begin{bmatrix} \boldsymbol{\varepsilon}^0 \\ \boldsymbol{\varepsilon}^0 \end{bmatrix}. \tag{4.7}$$

We note that the entries in the matrix equation above are fourth order and second order tensors. Solving (4.7) for $\boldsymbol{\varepsilon}_I^*$ and $\boldsymbol{\varepsilon}_E^*$ gives

$$\boldsymbol{\varepsilon}_I^* = [\mathbb{A}_E - \Delta\mathbb{S}] : \mathbb{M}^{-1} : \boldsymbol{\varepsilon}^0\,, \quad \boldsymbol{\varepsilon}_E^* = [\mathbb{A}_I - \Delta\mathbb{S}] : \mathbb{M}^{-1} : \boldsymbol{\varepsilon}^0, \tag{4.8}$$

with

$$\Delta\mathbb{S} := \langle\mathbb{S}^{I,C}\rangle_{\Omega_I} - \langle\mathbb{S}^{E,C}\rangle_{\Omega_E} \quad \left(= \langle\overline{\mathbb{S}}^{E,C}\rangle_{\Omega_E} - \langle\overline{\mathbb{S}}^{I,C}\rangle_{\Omega_I}\right), \tag{4.9.1}$$

$$\mathbb{M} := \left[\mathbb{A}_I - \langle\mathbb{S}^{I,C}\rangle_{\Omega_I}\right] : \left[\mathbb{A}_E - \langle\overline{\mathbb{S}}^{E,C}\rangle_{\Omega_E}\right] - \langle\overline{\mathbb{S}}^{I,C}\rangle_{\Omega_I} : \langle\mathbb{S}^{E,C}\rangle_{\Omega_E}. \tag{4.9.2}$$

We note that in (4.9.1) we have used the fact that $\mathbb{S}^{I,C}|_{f=1}$ is constant and we therefore have $\langle\mathbb{S}^{I,C}|_{f=1}\rangle_{\Omega_E} = \langle\mathbb{S}^{I,C}|_{f=1}\rangle_{\Omega_I}$. Further note that all tensor contractions above commute since we are considering isotropy.

The average strain in the two phases now follows from (4.5) and (4.8) as

$$\begin{aligned}\langle\boldsymbol{\varepsilon}\rangle_{\Omega_I} &:= \boldsymbol{\varepsilon}^0 + \langle\boldsymbol{\varepsilon}^d\rangle_{\Omega_I} = \mathbb{A}_I : \mathbb{B}_E : \boldsymbol{\varepsilon}^0\,, \quad \mathbb{B}_E := [\mathbb{A}_E - \Delta\mathbb{S}] : \mathbb{M}^{-1}\,,\\ \langle\boldsymbol{\varepsilon}\rangle_{\Omega_E} &:= \boldsymbol{\varepsilon}^0 + \langle\boldsymbol{\varepsilon}^d\rangle_{\Omega_E} = \mathbb{A}_E : \mathbb{B}_I : \boldsymbol{\varepsilon}^0\,, \quad \mathbb{B}_I := [\mathbb{A}_I - \Delta\mathbb{S}] : \mathbb{M}^{-1}\,,\end{aligned} \tag{4.10}$$

so that the average strain of both phases becomes

$$\langle\boldsymbol{\varepsilon}\rangle_\Omega = f\langle\boldsymbol{\varepsilon}\rangle_{\Omega_I} + (1-f)\langle\boldsymbol{\varepsilon}\rangle_{\Omega_E} = [f\ \mathbb{A}_I : \mathbb{B}_E + (1-f)\ \mathbb{A}_E : \mathbb{B}_I] : \boldsymbol{\varepsilon}^0\,. \tag{4.11}$$

On the other hand the average stress in the two phases is given by Eq. (4.2) which can be written as

$$\begin{aligned}\langle\boldsymbol{\sigma}\rangle_{\Omega_I} &= \widetilde{\mathbb{C}} : (\boldsymbol{\varepsilon}^0 + \langle\boldsymbol{\varepsilon}^d\rangle_{\Omega_I} - \boldsymbol{\varepsilon}_I^*) = \widetilde{\mathbb{C}} : [\mathbb{A}_I - \mathbb{I}^s] : \mathbb{B}_E : \boldsymbol{\varepsilon}^0\,,\\ \langle\boldsymbol{\sigma}\rangle_{\Omega_E} &= \widetilde{\mathbb{C}} : (\boldsymbol{\varepsilon}^0 + \langle\boldsymbol{\varepsilon}^d\rangle_{\Omega_E} - \boldsymbol{\varepsilon}_E^*) = \widetilde{\mathbb{C}} : [\mathbb{A}_E - \mathbb{I}^s] : \mathbb{B}_I : \boldsymbol{\varepsilon}^0\,,\end{aligned} \tag{4.12}$$

and therefore the average stress of both phases is

$$\begin{aligned}\langle\boldsymbol{\sigma}\rangle_{\Omega_I} &= f\langle\boldsymbol{\sigma}\rangle_{\Omega_I} + (1-f)\langle\boldsymbol{\sigma}\rangle_{\Omega_E}\\ &= \left[f\widetilde{\mathbb{C}} : [\mathbb{A}_I - \mathbb{I}^s] : \mathbb{B}_E + (1-f)\widetilde{\mathbb{C}} : [\mathbb{A}_E - \mathbb{I}^s] : \mathbb{B}_I\right] : \boldsymbol{\varepsilon}^0\,.\end{aligned} \tag{4.13}$$

The effective modulus $\overline{\mathbb{C}}$ of the two phase composite is defined by the relation

$$\langle\boldsymbol{\sigma}\rangle_\Omega = \overline{\mathbb{C}} : \langle\boldsymbol{\varepsilon}\rangle_\Omega\,, \tag{4.14}$$

from which follows

$$\begin{aligned}&\left[f\widetilde{\mathbb{C}} : [\mathbb{A}_I - \mathbb{I}^s] : \mathbb{B}_E + (1-f)\widetilde{\mathbb{C}} : [\mathbb{A}_E - \mathbb{I}^s] : \mathbb{B}_I\right] : \boldsymbol{\varepsilon}^0\\ &\quad = \overline{\mathbb{C}} : [f\mathbb{A}_I : \mathbb{B}_E + (1-f)\mathbb{A}_E : \mathbb{B}_I]^{-1} : \boldsymbol{\varepsilon}^0\,.\end{aligned} \tag{4.15}$$

Note that $\boldsymbol{\varepsilon}^0$ and the cumbersome tensor $\mathbb{M}^{-1}$ cancel. Expression (4.15) still does not admit $\widetilde{\mathbb{C}} = \mathbb{C}^I$ or $\widetilde{\mathbb{C}} = \mathbb{C}^E$ yet. However we can further pull out the tensors $\mathbb{A}_I$ and $\mathbb{A}_E$ on both sides. The final expression for the effective elastic modulus then becomes

$$\overline{\mathbb{C}} = \left[f\mathbb{C}^I : \mathcal{A}_E + (1-f)\mathbb{C}^E : \mathcal{A}_I\right] : \left[f\mathcal{A}_E + (1-f)\mathcal{A}_I\right]^{-1}, \tag{4.16}$$

with

$$\mathcal{A}_E = \mathbb{I}^s - \mathbb{A}_E^{-1} : \Delta\mathbb{S}, \quad \mathcal{A}_I = \mathbb{I}^s - \mathbb{A}_I^{-1} : \Delta\mathbb{S}. \tag{4.17}$$

The formula now admits the cases $\widetilde{\mathbb{C}} = \mathbb{C}^E$ or $\widetilde{\mathbb{C}} = \mathbb{C}^I$ which arise from setting $\boldsymbol{\varepsilon}_E^* = 0$ or $\boldsymbol{\varepsilon}_I^* = 0$. In terms of the effective bulk modulus $\bar{\kappa}$ and shear modulus $\bar{\mu}$ of the composite, Eq. (4.16) corresponds to

$$\bar{\kappa} = \frac{f\kappa^I\left(1-\left(1-\frac{\kappa_E}{\tilde{\kappa}}\right)\Delta s_1^C\right) + (1-f)\,\kappa^E\left(1-\left(1-\frac{\kappa_I}{\tilde{\kappa}}\right)\Delta s_1^C\right)}{f\left(1-\left(1-\frac{\kappa_E}{\tilde{\kappa}}\right)\Delta s_1^C\right) + (1-f)\left(1-\left(1-\frac{\kappa_I}{\tilde{\kappa}}\right)\Delta s_1^C\right)}, \tag{4.18.1}$$

$$\bar{\mu} = \frac{f\mu^I\left(1-\left(1-\frac{\mu_E}{\tilde{\mu}}\right)\Delta s_2^C\right) + (1-f)\mu^E\left(1-\left(1-\frac{\mu_I}{\tilde{\mu}}\right)\Delta s_2^C\right)}{f\left(1-\left(1-\frac{\mu_E}{\tilde{\mu}}\right)\Delta s_2^C\right) + (1-f)\left(1-\left(1-\frac{\mu_I}{\tilde{\mu}}\right)\Delta s_2^C\right)}, \tag{4.18.2}$$

where $\tilde{\kappa}$ and $\tilde{\mu}$ are the moduli of the comparison solid. Further Δs_1^C and Δs_2^C are the coefficients given explicitly in Eq. (A.15) by setting $\nu = \tilde{\nu}$ and $\mu = \tilde{\mu}$.

4.3 Four special cases

We now discuss the possible applications of Eq. (4.16) or (4.18), respectively:

1. Setting both $\boldsymbol{\varepsilon}_I^* = 0$ and $\boldsymbol{\varepsilon}_E^* = 0$ (i.e. $\widetilde{\mathbb{C}} = \mathbb{C}^I$ in Ω_I and $\widetilde{\mathbb{C}} = \mathbb{C}^E$ in Ω_E) gives $\mathbb{A}_I^{-1} = 0$ and $\mathbb{A}_E^{-1} = 0$. We therefore arrive at the Voigt bound $\overline{\mathbb{C}} = f\mathbb{C}^I + (1-f)\mathbb{C}^E$.
2. Similarly one can obtain the Reuss bound. We therefore need to consider the homogenization of the RVE in terms of an eigenstress $\boldsymbol{\sigma}^*$. We can then arrive at a formula for the compliance $\overline{\mathbb{D}}$ analogous to Eq. (4.16). (As long as $\widetilde{\mathbb{C}}$ is equal in both domains Ω_I and Ω_E this formula for $\overline{\mathbb{D}}$ will be equal to the inverse of $\overline{\mathbb{C}}$). For the same special case as above (i.e., $\widetilde{\mathbb{C}} = \mathbb{C}^I$ in Ω_I and $\widetilde{\mathbb{C}} = \mathbb{C}^E$ in Ω_E) the formula for $\overline{\mathbb{D}}$ specializes to the Reuss bound $\overline{\mathbb{D}} = f\,\mathbb{D}^I + (1-f)\,\mathbb{D}^E$.
3. Setting $\boldsymbol{\varepsilon}_E^* = 0$ gives the interior eigenstrain method as noted in Fig. 4 We then have $\widetilde{\mathbb{C}} = \mathbb{C}^E$ and thus $\mathbb{A}_E^{-1} = 0$. From Eq. (4.16) then follows that

   $$\overline{\mathbb{C}} = \mathbb{C}^E - f\mathbb{C}^E : \left[\mathbb{A}_I - (1-f)\,\Delta\mathbb{S}\right]^{-1}, \tag{4.19}$$

   where $\Delta\mathbb{S}$ takes the properties of the exterior phase Ω_E, since $\widetilde{\mathbb{C}} = \mathbb{C}^E$. Note that $\mathbb{A}_I = \left[\mathbb{C}^E - \mathbb{C}^I\right]^{-1} : \mathbb{C}^E$ here. Expression (4.19) is the modified Mori-Tanaka method as derived in [16]. It resorts to the original Mori-Tanaka method if an infinite RVE is considered so that $\langle\mathbb{S}^{E,\infty}\rangle_{\Omega E} = 0$ and thus $\Delta\mathbb{S} = \langle\mathbb{S}^{I,\infty}\rangle\rangle_{\Omega I}$. We note that (4.19) is equal to the modified Mori-Tanaka method reported in [19].

   If we consider a composite of two materials we are faced with two possibilities: (i) placing material 1 in Ω_E and material 2 in Ω_I, and (ii) the flipped case of placing material 2 in Ω_E and material 1 in Ω_I.
4. The exterior eigenstrain method is obtained by setting $\boldsymbol{\varepsilon}_I^* = 0$ so that $\widetilde{\mathbb{C}} = \mathbb{C}^I$ and thus $\mathbb{A}_E^{-1} = 0$. We thus obtain

   $$\overline{\mathbb{C}} = \mathbb{C}^I - (1-f)\mathbb{C}^I : \left[\mathbb{A}_E - f\,\Delta\mathbb{S}\right]^{-1}, \tag{4.20}$$

   where $\Delta\mathbb{S}$ takes the properties of the interior phase Ω_I, since $\widetilde{\mathbb{C}} = \mathbb{C}^I$. Note that $\mathbb{A}_E = \left[\mathbb{C}^I - \mathbb{C}^E\right]^{-1} : \mathbb{C}^I$ here. Expression (4.20) can be considered as the flip of the modified Mori-Tanaka formula (4.19), which arises when flipping the properties of Ω_I and Ω_E, i.e. flipping

$\mathbb{C}^I \leftrightarrow \mathbb{C}^E$ and $f_I \leftrightarrow f_E$. Equation (4.20) gives the flip of the original Mori-Tanaka method if considering an infinite RVE where $\langle \mathbb{S}^{E,\infty} \rangle \boldsymbol{\Omega}_E = 0$ and thus $\Delta \mathbb{S} = \langle \mathbb{S}^{I,\infty} \rangle_{\boldsymbol{\Omega}_I}$.

Again for two given materials 1 and 2 we are faced with two possible placing choices, denoted by (iii) and (iv) in the following.

The four cases discussed above are displayed in Fig. 6. Here we consider two materials with $\kappa_1 < \kappa_2$ and $\mu_1 < \mu_2$. The plots are normalized by κ_1 and μ_1. The material ratios are chosen as $\kappa_2 = 4\kappa_1$ and $\mu_2 = 10\mu_1$. Furthermore Poisson's ratio of either matrix or inclusion phase must be specified. Here we have chosen $\nu_1 = 0.4$ giving $\nu_2 = 0.2727$. Figure 6a shows the effective bulk modulus $\bar{\kappa}$, normalized by κ_1 and given by Eq. (4.18.1). The effective shear modulus $\bar{\mu}$, given by (4.18.2), is displayed in Figs. 6b and 6d. In Figs. 6a, 6b and 6d the two green curves show the Voigt and Reuss bounds according to cases 1 and 2 above. The modified Mori-Tanaka Method comes in two versions: the interior eigenstrain method (4.19) and the exterior eigenstrain method (4.20). Both depend on the shear modulus of the surrounding composite μ_c. Varying μ_c does not affect the bulk modulus $\bar{\kappa}$. Therefore Eqs. (4.19) and (4.20) only give the *two blue lines* shown in Fig. 6a. Here the lower blue line corresponds to the placements (i) and (iv), which are equal in case of the bulk modulus. On the other hand, the upper blue line corresponds to the placements (ii) and (iii), which are also equal here. In the deviatoric case, however, μ_c has a strong influence on the effective shear modulus $\bar{\mu}$. Furthermore placements (i) and (iv), and (ii) and (iii) now yield different results. Figure 6b displays the results obtained from Eq. (4.19), and Fig. 6d displays the results obtained from Eq. (4.19). Varying μ_c in (4.19) gives the two grey regions corresponding to placements (i) and

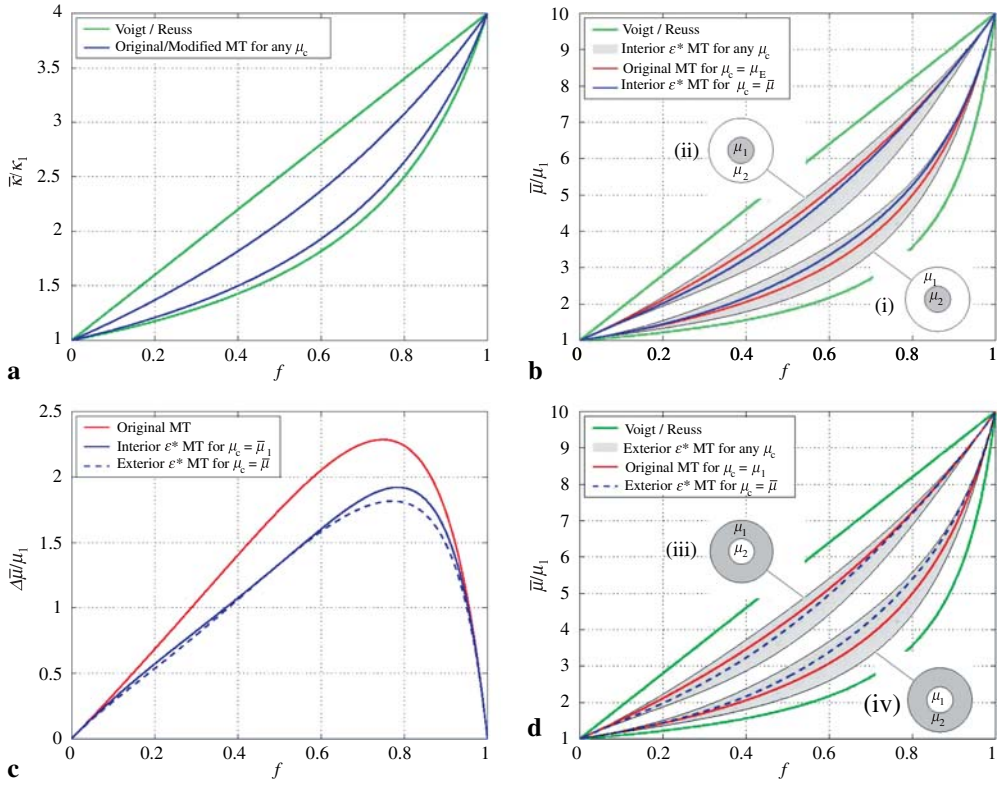

Fig. 6. **a** Effective bulk modulus; Effective shear modulus **b** for the interior and **d** for the exterior eigenstrain method; **c** Bandwidth of the shear bounds

(ii), while the variation of μ_c in (4.20) gives the two grey regions corresponding to placements (iii) and (iv). The upper boundary of the four grey regions is given by $\mu_c = \infty$ (the Dirichlet case) while the lower boundary is given by $\mu_c = 0$ (the Neumann limit.) The special case $\mu_c = \tilde{\mu}$, which corresponds to the original Mori-Tanaka result, is shown in *red*. (We note that the *red lines* of Figs. 6b and 6d agree exactly.) The *blue lines* show the case for $\mu_c = \bar{\mu}$, which is an implicit method. In Sect. 5 we consider the Hashin-Shtrikman bounds and we will see that the *red set of lines* above corresponds to the original Hashin-Shtrikman result. The *blue set of lines*, on the other hand, corresponds to a modified Hashin-Shtrikman result. It can be seen that these bounds are significantly tightened. Figures 6b and 6d look very alike and it is difficult to see much difference. Therefore in Fig. 6c we display the bandwidth (upper bound minus lower bound) of the original Mori-Tanaka (MT) method ($\mu_c = \tilde{\mu}$, in red) and the two modified MT methods (4.19) and (4.20) using $\mu_c = \bar{\mu}$. One can see that the new methods have considerably lower bandwidth as the original method and that there is a subtle difference between (4.19) and (4.20).

4.4 General cases

So far we have considered four special cases of the Dual Eigenstrain method. Let us now look at the general case where both $\boldsymbol{\varepsilon}_I^*$ and $\boldsymbol{\varepsilon}_E^*$ are nonzero. In other words $\widetilde{\mathbb{C}}$ is neither equal to $\mathbb{C}^I$ nor equal to $\mathbb{C}^E$. However, in the following, we restrict ourselves to $\widetilde{\mathbb{C}}$ being bounded by $\mathbb{C}^I$ and $\mathbb{C}^E$. Since the extreme cases $\widetilde{\mathbb{C}} = \mathbb{C}^I$ and $\widetilde{\mathbb{C}} = \mathbb{C}^E$ give the curves (i), (ii), (iii) and (iv) displayed in Fig. 6, we expect that an intermediate $\widetilde{\mathbb{C}}$ should also yield intermediate curves. It turns out that the Dual Eigenstrain (DE) method can be used to produce any curves between cases (i) and (iii), or between (ii) and (iv). In the following let us focus on the transition between (i) and (iii), i.e. the case where material 2 is located inside Ω_I and material 1 is located inside Ω_E. Let us further consider the choice $\mu_c = \tilde{\mu}$ (which produces a smooth transition between the original MT results shown in *red* in Fig. 6 (b) and (d)).

As a first application of the DE method let us consider the convex combination

$$\widetilde{\mathbb{C}} = a\mathbb{C}^I + (1-a)\mathbb{C}^E, \quad a \in [0,1]\,. \tag{4.21}$$

Figure 7 displays the effective bulk and shear moduli for $a = \{0.05, 0.15, 0.3, 0.5, 0.75\}$. We can see how the parameter a allows for a smooth transition between the interior eigenstrain method ($a = 0$) and the exterior eigenstrain method ($a = 1$), both shown in red. Since for an arbitrary isotropic composite, $\bar{\kappa}$ and $\bar{\mu}$ lie in between the bounds posed by $a = 1$ and $a = 0$, the DE method

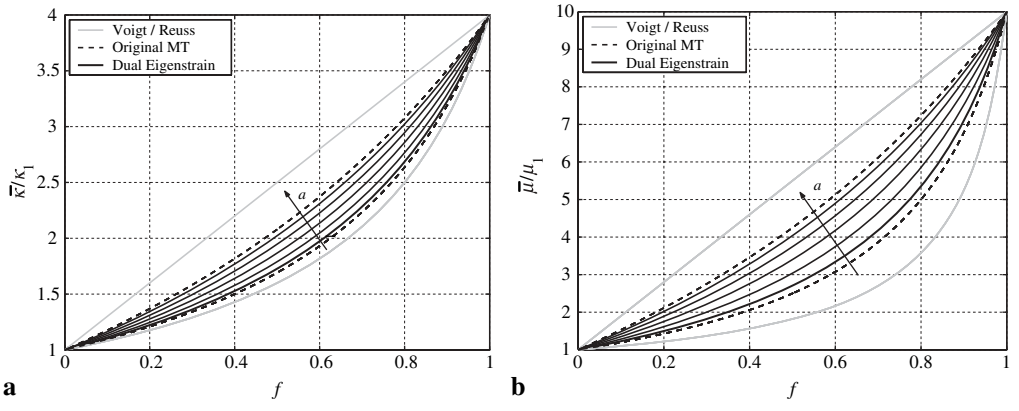

Fig. 7. Effective bulk **a** and shear modulus **b** using the dual eigenstrain method with the convex combination (4.21)

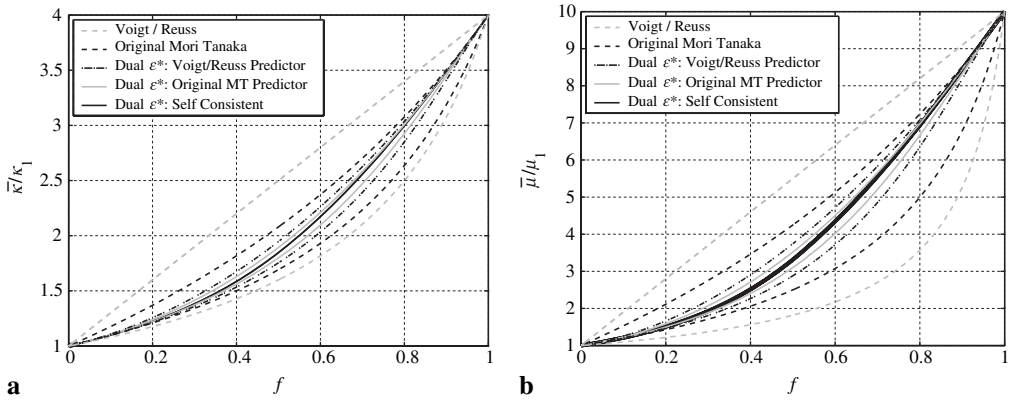

Fig. 8. Effective bulk **a** and shear modulus **b** using the dual eigenstrain method with various predictors

may be useful for curve fitting purposes of experimental data. We note that letting $a = a(f)$, i.e. a function of the volume fraction of the interior phase, any response between the interior and exterior eigenstrain methods can be produced.

As a second example of the DE let us consider $\widetilde{\mathbb{C}}$ to be predicted by some other homogenization scheme. For instance we have the Voigt and Reuss predictors

$$\begin{aligned} \widetilde{\mathbb{C}} &= f\mathbb{C}^I + (1-f)\mathbb{C}^E, \\ \widetilde{\mathbb{C}}^{-1} &= f\mathbb{C}^{I\,-1} + (1-f)\mathbb{C}^{E\,-1}, \end{aligned} \tag{4.22}$$

the original MT predictor, i.e. $\widetilde{\mathbb{C}}$ given by Eq. (4.19) $|_{\mu_c=\mu_E}$ or (4.20) $|_{\mu_c=\mu_I}$, and the Self Consistent predictor if we let $\widetilde{\mathbb{C}} = \overline{\mathbb{C}}$. Figure 8 shows the DE for the special cases $\widetilde{\mathbb{C}} = \mathbb{C}^I$ and $\widetilde{\mathbb{C}} = \mathbb{C}^E$ (both in red), and the five predictors given above. Here, as in Fig. 7, we have applied the Dual Eigenstrain method to the original Mori-Tanaka method, i.e., we have set $\mu_c = \tilde{\mu}$. The results of both Figs. 7 and 8 are qualitatively similar when considering other choices of μ_c, e.g., the Neumann case ($\mu_c = 0$), the self-consistent case ($\mu_c = \bar{\mu}$) or the Dirichlet case ($\mu_c = \infty$). Figure 8 shows that the plotted methods form a nested structure of subsequently narrower pairs. In particular the self consistent choice (the black line) of using $\tilde{\kappa} = \bar{\kappa}$ and $\mu_c = \tilde{\mu} = \bar{\mu}$ deserves further comment. It can be formally shown that this scheme gives exactly the same curve for all four placements (i) through (iv), and that furthermore this scheme is equivalent to the original Self Consistent scheme proposed by Hill [11], [12]. We can therefore conclude that the Dual Eigenstrain method unifies all the discussed homogenization schemes – i.e., the Voigt, Reuss, Original Mori-Tanaka, Luo and Weng's modified Mori-Tanaka, Hill's Self Consistent method, and, as we shall see, the Hashin-Shtrikman bounds – since they are all special cases of the DE method.

5 Modification of the Hashin-Shtrikman variational bounds

In this section we show how the Hashin-Shtrikman bounds are modified due to the Composite Eshelby tensors. Let us first consider the two special boundary conditions, the Dirichlet ($\mu_c = \infty$) and the Neumann Problem ($\mu_c = 0$). It is most appropriate to work with the principle of minimum potential energy (PMPE) when confronted with the Dirichlet problem. On the other hand, given the Neumann Problem, the principle of minimum complementary potential energy (PMCPE) is suitable. The respective results for these two special cases have been reported in [16]. Let us now consider the general case $\mu_c \in (0,\infty)$, for which neither the disturbance displacement field $\boldsymbol{u}^d$ nor the disturbance

traction field $\boldsymbol{t}^d$ can be supposed to vanish on the boundary of the RVE. To see how this affects the Hashin-Shtrikman bounds we construct the following modified Hashin-Shtrikman Variational Principle based on the PMPE.

Consider two comparable boundary value problems: First, the BVP of the heterogeneous composite RVE, characterized by a spatially varying modulus $\mathbb{C}(\boldsymbol{x})$ (as, for example, is shown in Fig. 1), and which is governed by the equations

$$\operatorname{div}\boldsymbol{\sigma} = 0\,, \quad \boldsymbol{\sigma} = \mathbb{C}(\boldsymbol{x}) : \boldsymbol{\varepsilon}\,, \quad \boldsymbol{\varepsilon} = \nabla^s \boldsymbol{u} \quad \text{in } \Omega \quad \boldsymbol{u} = \boldsymbol{\varepsilon}^0 \boldsymbol{x} + \bar{\boldsymbol{u}}^d \quad \text{on } \partial\Omega\,, \tag{5.1}$$

where $\bar{\boldsymbol{u}}^d$ is the prescribed value of the disturbance displacement field $\boldsymbol{u}^d$ on the RVE boundary, which is supposed to be non-zero in general. The value of $\bar{\boldsymbol{u}}^d$ can be determined from enforcing displacement continuity across the RVE/composite interface, as is considered in Sect. 3 by Eqs. (3.26) and (3.34.1). Second, let us consider the comparison BVP

$$\operatorname{div}\tilde{\boldsymbol{\sigma}} = 0\,, \quad \tilde{\boldsymbol{\sigma}} = \widetilde{\mathbb{C}} : \tilde{\boldsymbol{\varepsilon}}\,, \quad \tilde{\boldsymbol{\varepsilon}} = \nabla^s \tilde{\boldsymbol{u}} \quad \text{in } \Omega \tag{5.2.1}$$

$$\tilde{\boldsymbol{u}} = \left(\boldsymbol{\varepsilon}^0 + \langle \boldsymbol{\varepsilon}^d \rangle_\Omega\right) \boldsymbol{x} \quad \text{on } \partial\Omega, \tag{5.2.2}$$

which corresponds to a homogenized version of the first BVP, both in terms of the constant elastic modulus $\widetilde{\mathbb{C}}$ and in terms of the averaged boundary displacement. BVP (5.2) can be solved exactly and the solution is given by

$$\tilde{\mathbf{u}} = \tilde{\boldsymbol{\varepsilon}}\boldsymbol{x}, \quad \tilde{\boldsymbol{\varepsilon}} = \boldsymbol{\varepsilon}^0 + \langle \boldsymbol{\varepsilon}^d \rangle \Omega, \quad \forall \boldsymbol{x} \in \Omega, \tag{5.3}$$

where the strain $\tilde{\boldsymbol{\varepsilon}}$ is constant. The solution of the first BVP (5.1) can be expressed by the decomposition

$$\boldsymbol{u} = \boldsymbol{u}^0 + \boldsymbol{u}^d, \quad \boldsymbol{\varepsilon} = \boldsymbol{\varepsilon}^0 + \boldsymbol{\varepsilon}^d, \quad \forall \boldsymbol{x} \in \Omega, \tag{5.4.1,2}$$

where $\boldsymbol{u}^0 = \boldsymbol{\varepsilon}^0 \boldsymbol{x}$. The major idea of the particular choice of the comparison BVP is to ensure that the strain field solution of this BVP, $\tilde{\boldsymbol{\varepsilon}}$, is the average of the strain field solution of the composite BVP, $\boldsymbol{\varepsilon}$, i.e.,

$$\begin{aligned} &\boldsymbol{\varepsilon} = \nabla^s \mathbf{u} = \boldsymbol{\varepsilon}^0 + \boldsymbol{\varepsilon}^d, \\ &\tilde{\boldsymbol{\varepsilon}} = \nabla^s \tilde{\boldsymbol{\varepsilon}} = \boldsymbol{\varepsilon}^0 + \langle \boldsymbol{\varepsilon}^d \rangle = \langle \boldsymbol{\varepsilon} \rangle_\Omega. \end{aligned} \tag{5.5}$$

As is seen in Eq. (5.2.2) this is achieved by prescribing the average $\tilde{\boldsymbol{\varepsilon}}$ of the solution to the first BVP as a boundary condition on the second BVP. According to Eq. (5.5) the misfit in the strain field of the two BVP's is characterized by

$$\boldsymbol{\varepsilon} - \tilde{\boldsymbol{\varepsilon}} = \boldsymbol{\varepsilon}^d - \langle \boldsymbol{\varepsilon}^d \rangle_\Omega. \tag{5.6}$$

To characterize the misfit in the stress field between the composite and homogenized solid we define the stress polarization

$$\boldsymbol{p} := \boldsymbol{\sigma} - \widetilde{\mathbb{C}} : \boldsymbol{\varepsilon} = \Delta\mathbb{C} : \boldsymbol{\varepsilon}, \quad \Delta\mathbb{C} := \mathbb{C}(\boldsymbol{x}) - \widetilde{\mathbb{C}}. \tag{5.7}$$

From the equilibrium equation $\operatorname{div}\boldsymbol{\sigma} = 0$ of the first BVP follows (in component form)

$$(\widetilde{\mathbb{C}}_{ijk\ell}\varepsilon^d_{k\ell})_{,j} + p_{ij,j} = 0, \tag{5.8}$$

which is also termed the subsidiary condition. Let us now revisit the original Hashin-Shtrikman variational principle [6], [7], [10] for displacement boundary value problems. In the original formulation the quantity $\langle \boldsymbol{\varepsilon}^d \rangle_\Omega$ is zero and thus does not appear in the consideration of the comparison BVP. The solution of the comparison BVP is therefore characterized only by $\boldsymbol{\varepsilon}^0$ rather than by $\tilde{\boldsymbol{\varepsilon}} = \boldsymbol{\varepsilon}^0 + \langle \boldsymbol{\varepsilon}^d \rangle_\Omega$. Further, in the original formulation, the misfit in the strain field of the two BVP's is only given by $\boldsymbol{\varepsilon}^d$ rather than by $\boldsymbol{\varepsilon}^d - \langle \boldsymbol{\varepsilon}^d \rangle_\Omega$. In view of this we propose that the quantities

$\tilde{\boldsymbol{\varepsilon}}$ and $(\boldsymbol{\varepsilon}^d - \langle\boldsymbol{\varepsilon}^d\rangle_\Omega)$ should now play the roles that were formerly played by $\boldsymbol{\varepsilon}^0$ and $\boldsymbol{\varepsilon}^d$. We thus arrive at the following modified Hashin-Shtrikman variational principle:

Theorem (Modified Hashin-Shtrikman theorem): *Consider* $\mathbf{u}^d \in \mathcal{U}, \delta\mathbf{u}^d \in \mathcal{V}$ *and* $\boldsymbol{p} \in \mathcal{S}$, *where*

$$\begin{aligned}
\mathcal{U} &= \{\boldsymbol{u} | \boldsymbol{u} \in H^1(\Omega), \boldsymbol{u} = \langle\boldsymbol{\varepsilon}^d\rangle_\Omega \, \boldsymbol{x} \quad \text{on } \partial\Omega\}, \\
\mathcal{V} &= \{\boldsymbol{v} | \boldsymbol{v} \in H^1(\Omega), \boldsymbol{v} = \boldsymbol{0} \quad \text{on } \partial\Omega\}, \\
\mathcal{S} &= \{\boldsymbol{\sigma} | \boldsymbol{\sigma} \in L^2(\Omega)\}\,.
\end{aligned} \tag{5.9}$$

Then the potential $\Pi : \mathcal{S} \times \mathcal{U} \to \mathbb{R}$

$$\begin{aligned}
&\Pi = \widetilde{\Pi} - \frac{1}{2}\int_\Omega \left[\boldsymbol{p} : \Delta\mathbb{C}^{-1} : \boldsymbol{p} - \boldsymbol{p} : \left(\boldsymbol{\varepsilon}^d - \langle\boldsymbol{\varepsilon}^d\rangle_\Omega\right) - 2\boldsymbol{p} : \tilde{\boldsymbol{\varepsilon}}\right] dV, \\
&\textit{with} \quad \widetilde{\Pi} = \frac{1}{2}\int_\Omega \tilde{\boldsymbol{\varepsilon}} : \widetilde{\mathbb{C}} : \tilde{\boldsymbol{\varepsilon}}\; dV, \quad \Delta\mathbb{C} = \mathbb{C}(\boldsymbol{x}) - \widetilde{\mathbb{C}}\,, \quad \boldsymbol{p} = \Delta\mathbb{C} : \boldsymbol{\varepsilon},
\end{aligned} \tag{5.10}$$

satisfies the variational statements

$$\begin{aligned}
&1.\ \ \delta\Pi = 0 \iff (\widetilde{\mathbb{C}}_{ijk\ell}\varepsilon^d_{k\ell})_{,j} + p_{ij,j} = 0\,, \\
&2.\ \ \begin{array}{ll} \delta^2\Pi > 0\,, & \text{if } \Delta\mathbb{C} < 0 \ \ (pos.\,definite), \\ \delta^2\Pi < 0\,, & \text{if } \Delta\mathbb{C} > 0 \ \ (neg.\,definite). \end{array}
\end{aligned} \tag{5.11}$$

Proof First note that the variation of the constant $\tilde{\boldsymbol{\varepsilon}} = \langle\boldsymbol{\varepsilon}\rangle_\Omega = \boldsymbol{\varepsilon}^0 + \langle\boldsymbol{\varepsilon}^d\rangle_\Omega$ vanishes since

$$\delta\langle\varepsilon^d_{ij}\rangle_\Omega = \frac{1}{2V}\int_\Omega \left(\delta u^d_{i,j} + \delta u^d_{j,i}\right) dV = \frac{1}{2V}\int_{\partial\Omega} \left(\delta u^d_i\, n_j + \delta u^d_j\, n_i\right) dS = 0, \quad \forall\, \delta\boldsymbol{u}^d \in \mathcal{V}. \tag{5.12}$$

First statement: The variation of Π therefore becomes

$$\begin{aligned}
\delta\Pi &= -\frac{1}{2}\int_\Omega \left[2\delta\boldsymbol{p} : \Delta\mathbb{C}^{-1} : \boldsymbol{p} - \delta\boldsymbol{p} : (\boldsymbol{\varepsilon}^d - \langle\boldsymbol{\varepsilon}^d\rangle_\Omega) - \boldsymbol{p} : \delta\boldsymbol{\varepsilon}^d - 2\delta\boldsymbol{p} : \tilde{\boldsymbol{\varepsilon}}\right] dV \\
&= -\frac{1}{2}\int_\Omega \left[\delta\boldsymbol{p} : (\boldsymbol{\varepsilon}^d - \langle\boldsymbol{\varepsilon}^d\rangle_\Omega) - \boldsymbol{p} : \delta\boldsymbol{\varepsilon}^d\right] dV,
\end{aligned} \tag{5.13}$$

where we have used $\Delta\mathbb{C}^{-1} : \boldsymbol{p} = \boldsymbol{\varepsilon} = \tilde{\boldsymbol{\varepsilon}} + (\boldsymbol{\varepsilon}^d - \langle\boldsymbol{\varepsilon}^d\rangle_\Omega)$ according to Eq. (5.6) and (5.7). In view of the definition (5.7) and (5.1) we have $\boldsymbol{p} := \boldsymbol{\sigma} - \widetilde{\mathbb{C}} : (\boldsymbol{\varepsilon}^0 + \boldsymbol{\varepsilon}^d)$, thus $\delta\boldsymbol{p} = \delta\boldsymbol{\sigma} - \widetilde{\mathbb{C}} : \delta\boldsymbol{\varepsilon}^d$ and it follows that

$$\delta\Pi = -\frac{1}{2}\int_\Omega \left[\delta\boldsymbol{\sigma} : \left(\boldsymbol{\varepsilon}^d - \langle\boldsymbol{\varepsilon}^d\rangle_\Omega\right) - \boldsymbol{\sigma} : \delta\boldsymbol{\varepsilon}^d + \delta\boldsymbol{\varepsilon}^d : \widetilde{\mathbb{C}} : \tilde{\boldsymbol{\varepsilon}}\right] dV. \tag{5.14}$$

Since $\tilde{\boldsymbol{\sigma}} = \widetilde{\mathbb{C}} : \tilde{\boldsymbol{\varepsilon}}$ is a constant symmetric tensor the last contribution vanishes with the help of the divergence theorem, i.e.

$$\int_\Omega \delta\varepsilon^d_{ij}\, \tilde{\sigma}_{ij}\, dV = \int_\Omega \left(\delta u^d_i\, \tilde{\sigma}_{ij}\right)_{,j} dV = \int_{\partial\Omega} \delta u^d_i\, \tilde{\sigma}_{ij}\, n_j\, dS = 0, \quad \forall\ \delta\boldsymbol{u}^d \in \mathcal{V}. \tag{5.15}$$

By further use of the divergence theorem, the remaining part can be rewritten as

$$\begin{aligned}\delta\Pi &= -\frac{1}{2}\int\limits_{\partial\Omega}\left[\delta\sigma_{ij}\big(u_i^d - \langle\varepsilon_{ik}^d\rangle_{\Omega}x_k\big) - \sigma_{ij}\,\delta u_i^d\right]n_j\,dS \\ &\quad+\frac{1}{2}\int\limits_{\Omega}\Big[\delta\sigma_{ij,j}\Big(u_i^d - \langle\varepsilon_{ij}^d\rangle_{\Omega}\Big) - \sigma_{ij,j}\,\delta u_i^d\Big]\,dV.\end{aligned} \tag{5.16}$$

On the boundary $\partial\Omega$, we have $u_i^d = \langle\varepsilon_{ik}^d\rangle_{\Omega}\,x_k$ and $\delta u_i^d = 0$, so that $\delta\Pi = 0$ is satisfied iff $\sigma_{ij,j} \equiv 0$, which implies the subsidiary condition (5.8).

Second statement: Considering Eq. (5.12) and (5.13) the second variation of Π becomes

$$\begin{aligned}\delta^2\Pi &= -\int\limits_{\Omega}\left[\delta\boldsymbol{p} : \Delta\mathbb{C}^{-1} : \delta\boldsymbol{p} - \delta\boldsymbol{p} : \delta\boldsymbol{\varepsilon}^d\right]dV \\ &= -\int\limits_{\Omega}\Big[\delta\boldsymbol{p} : \Delta\mathbb{C}^{-1} : \delta\boldsymbol{p} + \delta\boldsymbol{\varepsilon}^d : \widetilde{\mathbb{C}} : \delta\boldsymbol{\varepsilon}^d\Big]\,dV,\end{aligned} \tag{5.17}$$

where we have used $\delta\boldsymbol{p} = \delta\sigma - \widetilde{\mathbb{C}} : \delta\boldsymbol{\varepsilon}^d$ and

$$\int\limits_{\Omega}\delta\sigma_{ij}\delta\varepsilon_{ij}^d\,dV = \int\limits_{\partial\Omega}\delta\sigma_{ij}\,\delta u_i^d\,n_j\,dS - \int\limits_{\Omega}\delta\sigma_{ij,j}\,\delta u_i^d\,dV = 0. \tag{5.18}$$

Clearly $\Delta\mathbb{C} > 0 \Rightarrow \delta^2\Pi < 0$. By virtue of (5.18), we obtain

$$\int\limits_{\Omega}\delta\boldsymbol{p} : \widetilde{\mathbb{C}}^{-1} : \delta\boldsymbol{p}\;dV = \int\limits_{\Omega}\Big[\delta\boldsymbol{\sigma} : \widetilde{\mathbb{C}}^{-1} : \delta\boldsymbol{\sigma} + \delta\boldsymbol{\varepsilon}^d : \widetilde{\mathbb{C}} : \delta\boldsymbol{\varepsilon}^d\Big]dV, \tag{5.19}$$

so that we further have

$$\begin{aligned}\delta^2\Pi &> -\int\limits_{\Omega}\Big[\delta\boldsymbol{p} : \Delta\mathbb{C}^{-1} : \delta\boldsymbol{p} + \delta\boldsymbol{p} : \widetilde{\mathbb{C}}^{-1} : \delta\boldsymbol{p}\Big]dV \\ &= -\int\limits_{\Omega}\delta\boldsymbol{p} : \Big(\widetilde{\mathbb{C}}^{-1} : \mathbb{C}(\boldsymbol{x}) : \Delta\mathbb{C}^{-1}\Big) : \delta\boldsymbol{p}\,dV,\end{aligned} \tag{5.20}$$

which yields $\Delta\mathbb{C} < 0 \Rightarrow \delta^2\Pi > 0$. □

We note that the theorem contains the original Hashin-Shtrikman variational principle as a special case when $\langle\boldsymbol{\varepsilon}^d\rangle_{\Omega} = 0$.

We now consider the homogenized RVE with effective elastic modulus $\overline{\mathbb{C}}$. The potential energy of the homogenized solid

$$\overline{\Pi} = \frac{1}{2}\int\limits_{\Omega}\tilde{\boldsymbol{\varepsilon}} : \overline{\mathbb{C}} : \tilde{\boldsymbol{\varepsilon}}\,dV \tag{5.21}$$

is bounded by

$$\Pi\big(\boldsymbol{p},\boldsymbol{\varepsilon}^d\big)\Big|_{\Delta\mathbb{C}\,>\,0} \le \inf_{\boldsymbol{\varepsilon}^d\epsilon\varepsilon}\overline{\Pi}\big(\boldsymbol{\varepsilon}^d\big) \le \Pi\big(\boldsymbol{p},\boldsymbol{\varepsilon}^d\big)\Big|_{\Delta\mathbb{C}<0}. \tag{5.22}$$

From this statement we derive the bounds for the effective bulk and shear moduli $\bar{\kappa}$ and $\bar{\mu}$ for an isotropic solid. To decouple the dilatational and deviatoric response let us consider the comparison strain $\tilde{\boldsymbol{\varepsilon}}$ and the polarization stress $\boldsymbol{p}$ to be of the form

$$\begin{matrix} p_{ij} = p\delta_{ij} + \tau\beta_{ij} \\ \tilde{\varepsilon}_{ij} = \tilde{\varepsilon}\delta_{ij} + \tilde{\gamma}\beta_{ij} \end{matrix}, \quad \delta_{ij} = \begin{cases} 1, & i = j \\ 0, & i \neq j \end{cases}, \quad \beta_{ij} = \begin{cases} 0, & i = j \\ 1, & i \neq j \end{cases} \tag{5.23}$$

We first apply the interior eigenstrain method to Eq. (5.22), where $\boldsymbol{\varepsilon}^*$ and thus $\boldsymbol{p}$ are nonzero only within Ω_I, i.e.

$$\boldsymbol{p}(\boldsymbol{x}) = \begin{cases} \boldsymbol{p} & \boldsymbol{x} \in \Omega_I, \\ 0 & \boldsymbol{x} \in \Omega_E. \end{cases} \tag{5.24}$$

Given the Composite Eshelby tensor $\mathbb{S}^{\bullet,C}$ of Box 3, all the terms in Eq. (5.22) can be directly evaluated without approximation: We first note that the stress polarization is related to the eigenstrain by $\boldsymbol{p} = -\widetilde{\mathbb{C}} : \boldsymbol{\varepsilon}^*$, so that in view of the Eshelby relation $\boldsymbol{\varepsilon}^d = \mathbb{S}^{\bullet,C} : \boldsymbol{\varepsilon}^*$ we have

$$\boldsymbol{\varepsilon}^d = -\mathbb{S}^{\bullet,C} : \widetilde{\mathbb{C}}^{-1} : \boldsymbol{p}. \tag{5.25}$$

Dividing by the volume $V = |\,\Omega\,|$ of the RVE the first four individual contributions to Eq. (5.22) become

$$\begin{aligned} &\frac{1}{V}\inf_{\boldsymbol{\varepsilon}^d \in \varepsilon} \overline{\Pi}(\boldsymbol{\varepsilon}^d) = \frac{9}{2}\bar{\kappa}\tilde{\varepsilon}^2 + 6\bar{\mu}\tilde{\gamma}^2, \\ &\frac{1}{V}\tilde{\Pi} = \frac{9}{2}\tilde{\kappa}\tilde{\varepsilon}^2 + 6\tilde{\mu}\tilde{\gamma}^2, \\ &\frac{1}{2V}\int_\Omega \boldsymbol{p} : \Delta\mathbb{C}^{-1} : \boldsymbol{p}\, dV = \frac{fp^2}{2(\kappa_I - \tilde{\kappa})} + \frac{3f\tau^2}{2(\mu_I - \tilde{\mu})}, \\ &\frac{1}{V}\int_\Omega \boldsymbol{p} : \tilde{\boldsymbol{\varepsilon}}\, dV = 3fp\tilde{\varepsilon} + 6f\tau\tilde{\gamma}. \end{aligned} \tag{5.26}$$

To evaluate the final contribution we employ the structure of the Composite Eshelby tensor given in Box 3. There we have

$$\boldsymbol{\varepsilon}^d = \alpha\boldsymbol{\varepsilon}^{d,D} + (1-\alpha)\boldsymbol{\varepsilon}^{d,N} + \beta\boldsymbol{\varepsilon}^{d,0} + \gamma\boldsymbol{\varepsilon}^{d,00}, \tag{5.27}$$

and since $\boldsymbol{\varepsilon}^{d,0}$, $\boldsymbol{\varepsilon}^{d,00}$ are constant and since $\langle\boldsymbol{\varepsilon}^{d,D}\rangle_\Omega = 0$ we obtain

$$\boldsymbol{\varepsilon}^d - \langle\boldsymbol{\varepsilon}^d\rangle_\Omega = \alpha\boldsymbol{\varepsilon}^{d,D} + (1-\alpha)(\boldsymbol{\varepsilon}^{d,N} - \langle\boldsymbol{\varepsilon}^{d,N}\rangle_\Omega). \tag{5.28}$$

In view of Eq. (5.25) the final piece in Eq. (5.22) gives

$$\frac{1}{2V}\int_\Omega \boldsymbol{p} : \boldsymbol{\varepsilon}^{d,D} dV = -\frac{1}{2V}\int_{\Omega_I} \boldsymbol{p} : \mathbb{S}^{I,D} : \widetilde{\mathbb{C}}^{-1} : \boldsymbol{p} dV = -\frac{f}{2}\boldsymbol{p} : \langle\mathbb{S}^{I,D}\rangle_{\Omega_I} : \widetilde{\mathbb{C}}^{-1} : \boldsymbol{p}, \tag{5.29}$$

and, since $\langle\mathbb{S}^{\bullet,N}\rangle_\Omega = f\mathbb{I}^s$,

$$\frac{1}{2V}\int_\Omega \boldsymbol{p} : (\boldsymbol{\varepsilon}^{d,N} - \langle\boldsymbol{\varepsilon}^{d,N}\rangle_\Omega) dV = -\frac{f}{2}\boldsymbol{p} : \left(\langle\mathbb{S}^{I,N}\rangle_{\Omega_I} - f\mathbb{I}^s\right) : \widetilde{\mathbb{C}}^{-1} : \boldsymbol{p}. \tag{5.30}$$

Combining the last two equations by using Eq. (5.28) we finally conclude for an isotopic material that

$$\frac{1}{2V}\int_\Omega \boldsymbol{p} : (\boldsymbol{\varepsilon}^d - \langle\boldsymbol{\varepsilon}^d\rangle_\Omega) dV = \frac{s_1^{HS} p^2}{2\tilde{\kappa}} + \frac{3s_2^{HS}\tau^2}{2\tilde{\mu}} \quad \text{with} \quad s_i^{HS} = \alpha s_i^{I,D} + (1-\alpha)(s_i^{I,N} - f), \quad i = 1,2, \tag{5.31}$$

and where $s_i^{I,D}$, $s_i^{I,N}$ are given in Appendix A. With Eqs. (5.26) and (5.31) all contributions of Π are specified and we can set the derivatives $\frac{\partial\Pi}{\partial p}$ and $\frac{\partial\Pi}{\partial\tau}$ equal to zero to obtain the two equations

$$\frac{p}{\kappa_I-\tilde{\kappa}}+\frac{s_1^{HS}p}{\tilde{\kappa}}-3\tilde{\varepsilon}=0,\quad \frac{\tau}{\mu_I-\tilde{\mu}}+\frac{s_2^{HS}\tau}{\tilde{\mu}}-2\tilde{\gamma}=0. \tag{5.32}$$

These can be solved for the stress polarization parameters p and τ. Plugging these into Π by considering the two choices $\tilde{\gamma}=0$ and $\tilde{\varepsilon}=0$ we find the two equations

$$\frac{\Pi}{V}=\frac{9\tilde{\varepsilon}^2}{2}\left(\tilde{\kappa}+\frac{f}{\frac{1}{\kappa_I-\tilde{\kappa}}+\frac{s_1^{HS}}{\tilde{\kappa}}}\right),\quad \frac{\Pi}{V}=\frac{6\tilde{\gamma}^2}{2}\left(\tilde{\mu}+\frac{f}{\frac{1}{\mu_I-\tilde{\mu}}+\frac{s_2^{HS}}{\tilde{\mu}}}\right). \tag{5.33}$$

We are now in the position to state the new Hashin-Shtrikman variational bounds. Let us consider two materials with $\kappa_1<\kappa_2$ and $\mu_1<\mu_2$. From Eq. (5.22) we now obtain

$$\begin{aligned}
&\kappa_1+\frac{f_2}{\frac{1}{\kappa_2-\kappa_1}+\frac{s_1^{HS}}{\kappa_1}}\le\bar{\kappa}\le\kappa_2+\frac{f_1}{\frac{1}{\kappa_1-\kappa_2}+\frac{s_1^{HS}}{\kappa_2}},\\
&\mu_1+\frac{f_2}{\frac{1}{\mu_2-\mu_1}+\frac{s_2^{HS}}{\mu_1}}\le\bar{\mu}\le\mu_2+\frac{f_1}{\frac{1}{\mu_1-\mu_2}+\frac{s_2^{HS}}{\mu_2}}.
\end{aligned} \tag{5.34}$$

Explicitly, for the value of α given in Eq. (3.28) we have

$$\begin{aligned}
s_1^{HS}&=\frac{1+\nu_1}{3(1-\nu_1)}f_1,\\
s_2^{HS}&=\frac{8-10\nu_1}{3(1-\nu_1)}f_1-21\ \frac{f_2\left(1-f_2^{\frac{2}{3}}\right)^2}{5(1-\nu_1)}\frac{2(\mu_c-\mu_1)}{4\mu_c(7-10\nu_1)+\mu_1(7+5\nu_1)},
\end{aligned} \tag{5.35}$$

for the lower bound, and

$$\begin{aligned}
s_1^{HS}&=\frac{1+\nu_2}{3(1-\nu_2)}f_2,\\
s_2^{HS}&=\frac{8-10\nu_2}{3(1-\nu_2)}f_2-21\frac{f_1(1-f_1^{\frac{2}{3}})^2}{5(1-\nu_2)}\frac{2(\mu_c-\mu_2)}{4\mu_c(7-10\nu_2)+\mu_2(7+5\nu_2)}
\end{aligned} \tag{5.36}$$

for the upper bound. It can be seen that s_1^{HS} is independent of μ_c, the stiffness of the surrounding composite, and that s_1^{HS} is equal to the corresponding expression of the original Hashin-Shtrikman formulation. Thus the bulk modulus bounds are identical to the original Hashin-Shtrikman bulk modulus bounds. For the shear modulus, however, the new bounds are different from the original solution. Since both expressions for s_2^{HS} depend on μ_c, the Hashin-Shtrikman shear bounds become explicitly dependent on the surrounding composite phase. In particular we note the special cases

$$\begin{aligned}
&1.\quad \mu_c=0 && \rightarrow \text{Neumann HS bounds},\\
&2.\quad \left\{\begin{matrix}\mu_c=\mu_1 & \text{for lower bound}\\ \mu_c=\mu_2 & \text{for upper bound}\end{matrix}\right\} && \rightarrow \text{Original HS bounds},\\
&3.\quad \mu_c=\infty && \rightarrow \text{Dirichlet HS bounds}.
\end{aligned} \tag{5.37}$$

The Dirichlet and Neumann special cases have been reported in [16]. It is known that the original HS bounds coincide with the original Mori-Tanaka method. Moreover it can be shown that the more general 'interior eigenstrain HS' bounds, given by (5.34)–(5.36), are identical to the 'interior eigenstrain modified Mori Tanaka' formula given in Eq. (4.19). Due to this equivalence, Fig. 6 also serves to illustrate the Hashin-Shtrikman bounds. In this figure we have used $\kappa_2=4\kappa_1$ and $\mu_2=10$ μ_1. The original HS bounds (in red) and the modified HS bounds for the implicit case $\mu_c=\bar{\mu}$ (in blue), are shown in Figs. 6a and 6b. (In case of the bulk modulus the original and modified HS bounds are

equal.) It can be seen that the modified Hashin-Shtrikman shear bounds, using $\mu_c = \bar{\mu}$ are substantially narrower than the original bounds. The grey regions in Fig. 6b marks the variation of the lower and upper Hashin-Shtrikman bounds for the possible range $0 < \mu_c < \infty$. The Neumann-Hashin-Shtrikman bounds ($\mu_c = 0$) are formed by the lower boundary of these grey regions while the Dirichlet-Hashin-Shrikman bounds ($\mu_c = \infty$) are formed by the upper boundary of the grey regions. It can thus be seen that the Neumann-HS bounds constitute a downward shift compared to the original HS bounds while the Dirichlet-HS bounds constitute an upward shift. This tendency can also be observed in the computational homogenization results obtained by Löhnert [17].

The bounds reported in Eqs. (5.34)–(5.36) are derived by considering the eigenstrain $\boldsymbol{\varepsilon}^*$ to be prescribed within Ω_I. Let us finally consider the case where $\boldsymbol{\varepsilon}^*$, and thus $\boldsymbol{p}$, is prescribed within Ω_E, i.e.

$$\boldsymbol{p}(\boldsymbol{x}) = \begin{cases} 0 & \boldsymbol{x} \in \Omega_I, \\ \boldsymbol{p} & \boldsymbol{x} \in \Omega_E. \end{cases} \tag{5.38}$$

Under this condition, termed the exterior eigenstrain method in Section 4, we can derive a second set of HS bounds. The relation between $\boldsymbol{\varepsilon}^d$ and $\boldsymbol{p}$ is now given by

$$\boldsymbol{\varepsilon}^d = -\overline{\mathbb{S}}^{\bullet,C} : \widetilde{\mathbb{C}}^{-1} : \boldsymbol{p}, \tag{5.39}$$

where $\overline{\mathbb{S}}^{\bullet,C}$ is given by Eq. (4.4). From here the derivation follows the same steps as above and is therefore omitted. The second set of bounds we obtain can also be expressed in the form (5.34) but where now

$$s_i^{HS} = -\alpha s_i^{E,D} - (1-\alpha)(s_i^{E,N} - f), \quad i = 1, 2. \tag{5.40}$$

Explicitly, by using (3.28), (A.11.2) and (A.12.2), this becomes

$$\begin{aligned} s_1^{HS} &= \frac{1+\nu_1}{3(1-\nu_1)} f_1, \\ s_2^{HS} &= \frac{8-10\nu_1}{3(1-\nu_1)} f_1 - \frac{42 f_1^2 \left(1 - f_1^{\frac{2}{3}}\right)^2}{5 f_2 (1-\nu_1)} \frac{\mu_c - \mu_1}{4\mu_c(7-10\nu_1) + \mu_1(7+5\nu_1)}, \end{aligned} \tag{5.41}$$

for the lower bound, and

$$\begin{aligned} s_1^{HS} &= \frac{1+\nu_2}{3(1-\nu_2)} f_2, \\ s_2^{HS} &= \frac{8-10\nu_2}{3(1-\nu_2)} f_2 - \frac{42 f_2^2 \left(1 - f_2^{\frac{2}{3}}\right)^2}{5 f_1 (1-\nu_2)} \frac{\mu_c - \mu_2}{4\mu_c(7-10\nu_2) + \mu_2(7+5\nu_2)}, \end{aligned} \tag{5.42}$$

for the upper bound. It can be shown that the 'exterior eigenstrain HS' bounds given by Eqs. (5.34), (5.41) and (5.42) are identical to the 'exterior eigenstrain MT' formula (4.20). The original HS bounds and the modified 'exterior eigenstrain HS' shear bounds for the parameters $\kappa_2 = 4\kappa_1$ and $\mu_2 = 10\mu_1$ are thus shown by the red and blue curves in Fig. 6d. For the bulk bounds the modified and original HS bounds are identical and are as shown in Fig. 6a

In the following let us denote the shear modulus bounds of the interior HS method by $\mu_\ell^I \le \bar{\mu} \le \mu_u^I$ and the shear modulus bounds of the exterior HS method by $\mu_\ell^E \le \bar{\mu} \le \mu_u^E$. Since the two sets of bounds are both valid we can combine them and write

$$\max\left(\mu_\ell^I, \mu_\ell^E\right) \le \bar{\mu} \le \min\left(\mu_u^I, \mu_u^E\right). \tag{5.43}$$

From Fig. 6c one can see that the exterior eigenstrain HS gives the narrowest bounds for the chosen material parameters ($\kappa_2/\kappa_1 = 4$, $\mu_2/\mu_1 = 10$ and $\nu_1 = 0.4$). For this case the modified HS bounds are up to 25% tighter than the original bounds.

We conclude this section on the remark that no approximations, as are needed in the derivation of the original HS bounds [30], are made here. Moreover, the new bounds derived here are significantly narrower than the original bounds.

6 Conclusions

This work serves three major purposes: First, in Sects. 2 and 3, we have derived the Composite Eshelby tensor $\mathbb{S}^{\bullet,C}$. It is the solution of the general Micromechanical BVP and it is summarized in Box 3. We then showed that the parameters α, β and γ can be found by placing the RVE within a surrounding medium with stiffness κ_c and μ_c and imposing the continuity of both the traction and displacement fields. Secondly, we have introduced the Dual Eigenstrain method, which unifies previous homogenization schemes. In particular it unifies the Voigt-, Reuss-, original Mori-Tanaka-, Luo and Weng's Mori-Tanaka- and Hill's Self Consistent scheme. Thirdly we have shown that the Hashin-Shtrikman bounds are modified due to the new Composite Eshelby Tensor, since it captures the elastic disturbance fields more precisely than the original, infinite Eshelby tensor. In particular, for the optimal choice $\bar{\mu} = \mu_c$ we can show that the Hashin-Shtrikman shear bounds are significantly tightened.

The Composite Eshelby tensor is a convenient tool to use. The derivation of the Dual Eigenstrain method and the modified Hashin-Shtrikman bounds are straightforward and do not require any approximations, such as where employed in the original derivations of Hashin-shtrikman principles. We therefore believe that the Composite Eshelby tensor is an important contribution, especially since homogenization techniques and variational bounds are widely used in material modelling.

Further extensions to this work could be the consideration of an RVE whose phases are not concentrically aligned. It may also be interesting to study the generalization to non constant eigenstrains $\boldsymbol{\varepsilon}^*$, which, for radially symmetric problems, should admit the same radial isotropic structure as the Composite Eshelby tensor.

Appendix A

List of coefficients

In this Appendix we list all the radial basis arrays needed to construct the Eshelby tensors $\mathbb{S}^{\bullet,*}$, $\mathbb{U}^{\bullet,*}$ and $\mathbb{T}^{\bullet,*}$ as given in Boxes 1, 2 and 3. The coefficients of the Infinite Eshelby tensor are

$$\mathbf{S}^{I,\infty}(t) = \frac{1}{15(1-\nu)}\begin{bmatrix} 5\nu-1 \\ 4-5\nu \\ 0 \\ 0 \\ 0 \\ 0 \end{bmatrix}, \quad \mathbf{S}^{E,\infty}(t) = \frac{\rho_0^3/t^3}{30(1-\nu)}\begin{bmatrix} 3\rho_0^2/t^2+10\nu-5 \\ 3\rho_0^2/t^2-10\nu+5 \\ 15(1-\rho_0^2/t^2) \\ 15(1-2\nu-\rho_0^2/t^2) \\ 15(\nu-\rho_0^2/t^2) \\ 15(7\rho_0^2/t^2-5) \end{bmatrix}, \tag{A.1}$$

$$\mathbf{U}^{I,\infty}(t) = \frac{H_0 t}{15(1-\nu)}\begin{bmatrix} 5\nu-1 \\ 4-5\nu \\ 0 \end{bmatrix}, \quad \mathbf{U}^{E,\infty}(t) = \frac{\rho_0^3 H_0/t^2}{30(1-\nu)}\begin{bmatrix} 3\rho_0^2/t^2+10\nu-5 \\ 3\rho_0^2/t^2-10\nu+5 \\ 15-15\rho_0^2/t^2 \end{bmatrix}, \tag{A.2}$$

and

$$\mathbf{T}^{I,\infty}(t) = \frac{2\mu}{15(1-\nu)} \begin{bmatrix} (1-12\nu+5\nu^2)/(2\nu-1) \\ 4-5\nu \\ 0 \end{bmatrix},$$
$$\mathbf{T}^{E,\infty}(t) = \frac{\mu\ \rho_0^3/t^3}{15(1-\nu)} \begin{bmatrix} -12\rho_0^2/t^2 + 10(1-\nu) \\ -12\rho_0^2/t^2 + 5(1+\nu) \\ 60(\rho_0^2/t^2 - 1) \end{bmatrix}. \tag{A.3}$$

The contributions from the Dirichlet boundary are

$$\mathbf{S}^{B,D}(t) = -\frac{\rho_0^3}{15(1-\nu)} \begin{bmatrix} 5\nu-1 \\ 4-5\nu \\ 0 \\ 0 \\ 0 \\ 0 \end{bmatrix} + \frac{\rho_0^3(1-\rho_0^2)}{20(1-\nu)(7-10\nu)} \begin{bmatrix} 2(7-10\nu t^2) \\ 7(5t^2-3)-20\nu t^2 \\ -10t^2(7-10\nu) \\ -40\nu t^2 \\ 30\nu t^2 \\ 0 \end{bmatrix}, \tag{A.4}$$

$$\mathbf{U}^{B,D}(t) = -\frac{\rho_0^3 H_0 t}{15(1-\nu)} \begin{bmatrix} 5\nu-1 \\ 4-5\nu \\ 0 \end{bmatrix} + \frac{\rho_0^3(1-\rho_0^2)H_0 t}{20(1-\nu)(7-10\nu)} \begin{bmatrix} 2(7-10\nu t^2) \\ 7(5t^2-3)-20\nu t^2 \\ -10t^2(7-10\nu) \end{bmatrix}, \tag{A.5}$$

and

$$\mathbf{T}^{B,D}(t) = -\frac{2\mu\ \rho_0^3}{15(1-\nu)} \begin{bmatrix} \dfrac{1-12\nu+5\nu^2}{2\nu-1} \\ 4-5\nu \\ 0 \end{bmatrix} + \frac{\mu\ \rho_0^3(1-\rho_0^2)}{10(1-\nu)(7-10\nu)} \begin{bmatrix} 2(7+5\nu t^2) \\ 7(5t^2-3)+10\nu t^2 \\ 10t^2(7-5\nu) \end{bmatrix}. \tag{A.6}$$

Further, from the Neumann boundary we get

$$\mathbf{S}^{B,N}(t) = \frac{\rho_0^3}{30(1-\nu)} \begin{bmatrix} 2-10\nu \\ 7-5\nu \\ 0 \\ 0 \\ 0 \\ 0 \end{bmatrix} - \frac{\rho_0^3(1-\rho_0^2)}{5(1-\nu)(7+5\nu)} \begin{bmatrix} 2(7-10\nu t^2) \\ 7(5t^2-3)-20\nu t^2 \\ -10t^2(7-10\nu) \\ -40\nu t^2 \\ 30\nu t^2 \\ 0 \end{bmatrix}, \tag{A.7}$$

$$\mathbf{U}^{B,N}(t) = \frac{\rho_0^3 H_0 t}{30(1-\nu)} \begin{bmatrix} 2-10\nu \\ 7-5\nu \\ 0 \end{bmatrix} - \frac{\rho_0^3(1-\rho_0^2)H_0 t}{5(1-\nu)(7+5\nu)} \begin{bmatrix} 2(7-10\nu t^2) \\ 7(5t^2-3)-20\nu t^2 \\ -10t^2(7-10\nu) \end{bmatrix}, \tag{A.8}$$

and

$$\mathbf{T}^{B,N}(t) = -\frac{\mu\ \rho_0^3}{15(1-\nu)} \begin{bmatrix} 2(1+5\nu) \\ 7-5\nu \\ 0 \end{bmatrix} - \frac{2\mu\ \rho_0^3(1-\rho_0^2)}{5(1-\nu)(7+5\nu)} \begin{bmatrix} 2(7+5\nu t^2) \\ 7(5t^2-3)+10\nu t^2 \\ 10t^2(7-5\nu) \end{bmatrix}. \tag{A.9}$$

Associated with the eigenstrain $\boldsymbol{\varepsilon}^*$ we have the traction array

$$\mathbf{T}^*(t) = \mathbf{K}_1 \mathbf{I}^s = \frac{1}{1-2\nu} \begin{bmatrix} 2\nu \\ 1-2\nu \\ 0 \end{bmatrix}. \tag{A.10}$$

When we average the Finite Eshelby tensors according to Eqs. (3.37) and (3.41) we find

$$s_1^{I,D} = \frac{(1+\nu)(1-f)}{3(1-\nu)}, \quad s_2^{I,D} = \frac{2(4-5\nu)(1-f)}{15(1-\nu)} - 21\gamma_u(1-f^{2/3}), \tag{A.11.1,2}$$

$$s_1^{E,D} = -\frac{(1+\nu)f}{3(1-\nu)}, \quad s_2^{E,D} = -\frac{2(4-5\nu)f}{15(1-\nu)} + 21\gamma_u f\frac{1-f^{2/3}}{1-f}, \tag{A.11.3,4}$$

and

$$s_1^{I,N} = \frac{1+\nu+2(1-2\nu)f}{3(1-\nu)}, \quad s_2^{I,N} = \frac{2(4-5\nu)+(7-5\nu)f}{15(1-\nu)} + 21\gamma_t(1-f^{2/3}), \tag{A.12.1,2}$$

$$s_1^{E,N} = \frac{2(1-2\nu)f}{3(1-\nu)}, \quad s_2^{E,N} = \frac{(7-5\nu)f}{15(1-\nu)} - 21\gamma_t f\frac{1-f^{2/3}}{1-f}, \tag{A.12.3,4}$$

with

$$\gamma_u = \frac{f(1-f^{2/3})}{10(1-\nu)(7-10\nu)}, \quad \gamma_t = \frac{4f(1-f^{2/3})}{10(1-\nu)(7+5\nu)}. \tag{A.13}$$

The differences between these coefficients are

$$\begin{aligned}
\Delta s_1^D &:= s_1^{I,D} - s_1^{E,D} = \frac{1+\nu}{3(1-\nu)}, \\
\Delta s_1^N &:= s_1^{I,N} - s_1^{E,N} = \frac{1+\nu}{3(1-\nu)}, \\
\Delta s_2^D &:= s_2^{I,D} - s_2^{E,D} = \frac{2(4-5\nu)}{15(1-\nu)} - 21\gamma_u\frac{1-f^{2/3}}{1-f}, \\
\Delta s_2^N &:= s_2^{I,N} - s_2^{E,N} = \frac{2(4-5\nu)}{15(1-\nu)} + 21\gamma_t\frac{1-f^{2/3}}{1-f}.
\end{aligned} \tag{A.14}$$

Furthermore we have

$$\begin{aligned}
\Delta s_1^C &:= s_1^{I,C} - s_1^{E,C} = \frac{1+\nu}{3(1-\nu)}, \\
\Delta s_2^C &:= s_2^{I,C} - s_2^{E,C} = \frac{2(4-5\nu)}{15(1-\nu)} + \frac{42f(1-f^{2/3})^2}{5(1-\nu)(1-f)}\frac{\mu-\mu_c}{4\mu_c(7-10\nu)+\mu(7+5\nu)}.
\end{aligned} \tag{A.15}$$

Acknowledgments

This work is supported by a grant from National Science Foundation (Grant No. CMS-0239130), which is greatly appreciated.

References

[1] Chiu, Y. P.: On the stress field due to initial strains in cuboid surrounded by an infinite elastic space. J. Appl. Mech. **44**, 587–590 (1977).

[2] Christensen, R. M., Lo, K. H.: Solutions for the effective shear properties in three phase sphere and cylinder models. J. Mech. Phys. Solids **27**, 315–330 (1979).

[3] Eshelby, J. D.: The determination of the elastic field of an ellipsoidal inclusion, and related problems. Proc. Roy. Soc. A **241**, 376–396 (1957).

[4] Eshelby, J. D.: The elastic field outside an ellipsoidal inclusion. Proc. Roy. Soc. A **252**, 561–569 (1959).

[5] Eshelby, J. D.: Elastic inclusions and inhomogeneities. In: Progress in solid mechanics, Vol. 2. pp. 89–104 (Snedden, N. I., Hill, R., eds.). North-Holland 1961.
[6] Hashin, Z., Shtrikman, S.: On some variational principles in anisotropic and nonhomogeneous elasticity. J. Mech. Phys. Solids **10**, 335–342 (1962a).
[7] Hashin, Z., Shtrikman, S.: A variational approach to the theory of the elastic behavior of polycrystals. J. Mech. Phys. Solids **10**, 343–352 (1962b).
[8] Hashin, Z.: The spherical inclusion with imperfect interface. J. Appl. Mech. **58**, 444–449 (1991).
[9] Hashin, Z.: The interphase/imperfect interface in elasticity with application to coated fiber composites. J. Mech. Phys. Solids **50**, 2509–2537 (2002).
[10] Hill, R.: New derivations of some elastic extremum principles. In: Progress in applied mechanics – The Prager anniversary volume, pp. 99–106. New York: Macmillan 1963.
[11] Hill, R.: Continuum micro-mechanics of elastoplastic polycrystals. J. Mech. Phys. Solids **13**, 89–101 (1965a).
[12] Hill, R.: Theory of mechanical properties of fibre-strengthened materials III. Self-consistent model. J. Mech. Phys. Solids **13**, 189–198 (1965b).
[13] Jiang, B., Weng, G. J.: A generalized self-consistent polycrystal model for the yield strength of nanocrystalline materials. J. Mech. Phys. Solids **52**, 1125–1149 (2004).
[14] Li, S., Sauer, R., Wang, G.: A circular inclusion in a finite domain. I. The Dirichlet-Eshelby problem. Acta Mech. **179**, 67–90 (2005).
[15] Li, S., Sauer, R. A., Wang, G.: The Eshelby tensors in a finite spherical domain: I. Theoretical formulations. J. Appl. Mech. **74**, 770–783 (2007a).
[16] Li, S., Wang, G., Sauer, R. A.: The Eshelby tensors in a finite spherical domain: II. Applications in homogenization. J. Appl. Mech. **74**, 784–797 (2007b).
[17] Löhnert, S.: Computational homogenization of microheterogeneous materials at finite strains including damage. Dissertation, Universität Hannover 2004.
[18] Luo, H. A., Weng, G. J.: On Eshelby's inclusion problem in a three-phase spherically concentric solid, and a modification of Mori-Tanaka's Method. Mech. Mater. **6**, 347–361 (1987).
[19] Luo, H. A., Weng, G. J.: On Eshelby's S-tensor in a three-phase cylindrical concentric solid and the elastic moduli of fibre-reinforced composites. Mech. Mater. **8**, 77–88 (1989).
[20] Marur, P. R.: Effective elastic moduli of syntactic foams. Mat. Lett. **59**, 1954–1957 (2005).
[21] Mura, T., Kinoshita, N.: The polynomial eigenstrain problem or an anisotropic ellipsoidal inclusion. Phys. Status Solidi A **48**, 447–450 (1978).
[22] Mura, T.: Micromechanics of defects in solids, 2nd ed. Boston: Martinus Nijhoff 1987.
[23] Nemat-Nasser, S., Hori, M.: Micromechanics: overall properties of heterogeneous materials, 2nd ed. Amsterdam: Elsevier 1999.
[24] Qiu, Y. P., Weng, G. J.: Elastic moduli of thickly coated particle and fiber-reinforced composites. J. Appl. Mech. **58**, 388–398 (1991).
[25] Rodin, G. J.: Eshelby's inclusion problem for polygons and polyhedra. J. Mech. Phys. Solids **44**, 1977–1995 (1996).
[26] Saidi, F., Bernabé, Y., Reuschlé, T.: Uniaxial compression of synthetic, poorly consolidated granular rock with a bimodal grain-size distribution. Rock Mech. Rock Engng. **38**, 129–144 (2005).
[27] Sharma, P., Ganti, S.: Size-dependent Eshelby's tensor for embedded nano-inclusions incorporating surface/interface energies. J. Appl. Mech. **71**, 663–671 (2004).
[28] Somigliana, C.: Sopra l'equilibrio di un corpo elastico isotropo, pp. 17–19. Il Nuovo Ciemento 1886.
[29] Wang, G., Li, S., Sauer, R.: A circular inclusion in a finite domain. II. The Neumann–Eshelby problem. Acta Mech. **179**, 91–110 (2005).
[30] Willis, J. R.: Variational and related methods for the overall properties of composites. In: Advances in applied mechanics (Yih, C.-S., ed.). Vol. 21, pp. 1–78. New York: Academic Press 1981.